4

Planar Kinematics

If all links of a mechanical system undergo motion in one plane or in parallel planes, the system is said to be experiencing *planar motion*. In this chapter, only *planar mechanisms,* in which all links experience planar motion, are considered. A more descriptive explanation of conditions for planar motion is given in Chap. 9.

In Chap. 3 several examples of kinematic analyses were given using a minimal set of Lagrangian coordinates. Kinematic analysis of mechanical systems using Cartesian coordinates is no different in principle from the method of analysis with Lagrangian coordinates. The use of Cartesian coordinates, however, results in a larger number of coordinates and constraint equations. The number of degrees of freedom of a system, however, is the same regardless of the type of coordinates used. Since the number of independent coordinates is equal to the number of degrees of freedom of a system, then the number of dependent Cartesian coordinates is generally greater than the number of dependent Lagrangian coordinates.

Cartesian coordinates are used exclusively in this chapter and the remainder of the text.

4.1 CARTESIAN COORDINATES

In order to specify the configuration or state of a planar mechanical system, it is first necessary to define coordinates that specify the location of each body. Let the xy coordinate system shown in Fig. 4.1 be a global reference frame. Define a body-fixed $\xi_i\eta_i$ coordinate system embedded in body i. Body i can be located in the plane by specifying the global coordinates $\mathbf{r}_i = [x, y]_i^T$ of the origin of the body-fixed coordinate system and the angle ϕ_i of rotation of this system relative to the global coordinate system. This angle is considered positive if the rotation from positive x axis to positive ξ_i axis is counterclockwise.

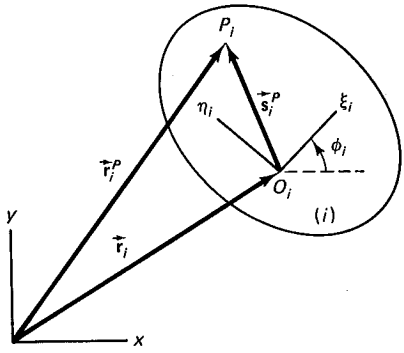

Figure 4.1 Locating point P relative to the body-fixed and global coordinate systems.

A point P_i on body i can be located from the origin of the $\xi_i\eta_i$ axes by the vector $\vec{s}_i^P$. The coordinates of point P_i with respect to the $\xi_i\eta_i$ coordinate system are ξ_i^P and η_i^P. The local (body-fixed) components of vector $\vec{s}_i^P$ are shown as $\mathbf{s}'^P_i = [\xi^P, \eta^P]_i^T$. Since P_i is a fixed point on body i, ξ_i^P and η_i^P are constants, and therefore $\mathbf{s}'^P_i$ is a constant vector. The global xy components of vector $\vec{s}_i^P$ are shown as $\mathbf{s}_i^P$. The elements of $\mathbf{s}_i^P$ vary when body i rotates. Point P_i may also be located by its global coordinates $\mathbf{r}_i^P = [x^P, y^P]_i^T$. It is clear that the components of $\vec{r}_i^P$ are not necessarily constant, since body i may be in motion. Position vectors such as $\mathbf{r}_i^P$, $\mathbf{s}_i^P$, $\mathbf{s}'^P_i$, $\mathbf{r}_i$, and so forth, are 3-vectors. However, in planar motion, since the z component of these vectors remains constant, the vectors are treated as 2-vectors.

The relation between the local and global coordinates of point P_i is

$$\mathbf{r}_i^P = \mathbf{r}_i + \mathbf{A}_i\mathbf{s}'^P_i \tag{4.1}$$

where

$$\mathbf{A}_i = \begin{bmatrix} \cos\phi & -\sin\phi \\ \sin\phi & \cos\phi \end{bmatrix}_i \tag{4.2}$$

is the rotational transformation matrix for body i. The transformation matrix $\mathbf{A}_i$ is the simplified form of the following 3×3 matrix:

$$\mathbf{A}_i = \begin{bmatrix} \cos\phi & -\sin\phi & 0 \\ \sin\phi & \cos\phi & 0 \\ 0 & 0 & 1 \end{bmatrix}_i$$

Equation 4.1 in expanded form can be written as

$$\begin{bmatrix} x^P \\ y^P \end{bmatrix}_i = \begin{bmatrix} x \\ y \end{bmatrix}_i + \begin{bmatrix} \cos\phi & -\sin\phi \\ \sin\phi & \cos\phi \end{bmatrix}_i \begin{bmatrix} \xi^P \\ \eta^P \end{bmatrix}_i$$

or

$$\begin{aligned} x_i^P &= x_i + \xi_i^P \cos\phi_i - \eta_i^P \sin\phi_i \\ y_i^P &= y_i + \xi_i^P \sin\phi_i + \eta_i^P \cos\phi_i \end{aligned} \tag{4.3}$$

Note that

$$\mathbf{s}_i^P = \mathbf{A}_i\mathbf{s}'^P_i \tag{4.4}$$

is the relationship between the local and global components of vector $\vec{s}_i^P$.

The vector of coordinates for body i is denoted by the vector

$$\begin{aligned}\mathbf{q}_i &= [\mathbf{r}^T, \phi]_i^T \\ &= [x, y, \phi]_i^T \end{aligned} \tag{4.5}$$

For a mechanical system with b bodies, the coordinate vector is the $3 \times b$ vector

$$\begin{aligned}\mathbf{q} &= [\mathbf{q}_1^T, \mathbf{q}_2^T, \ldots, \mathbf{q}_b^T]^T \\ &= [x_1, y_1, \phi_1, x_2, y_2, \phi_2, \ldots, x_b, y_b, \phi_b]^T \end{aligned} \tag{4.6}$$

where $\mathbf{q}$ without a subscript denotes the vector of coordinates for the entire system.

An algebraic 3-vector *with* a superscript prime is one that contains local components; e.g., $\mathbf{s}_i'^P$, $\mathbf{s}_j'$, $\mathbf{n}_j'$, or $\boldsymbol{\omega}_i'$. An algebraic 3-vector *without* a superscript prime is one that contains global components; e.g., $\mathbf{s}_i^P$, $\mathbf{s}_j$, $\mathbf{n}_j$, $\boldsymbol{\omega}_j$, $\mathbf{r}_i^P$, or $\mathbf{r}_j$.

Example 4.1

For the mechanism shown in the illustration, body 3 has translational coordinates $\mathbf{r}_3 = [1.2, 2.5]^T$ and $\phi_3 = 5.67$ rad. Point B on body 3 has local coordinates $\xi_3^B = -1.8$ and $\eta_3^B = 1.3$. Find the global components of vector $\vec{s}_3^B$ and the global coordinates of B.

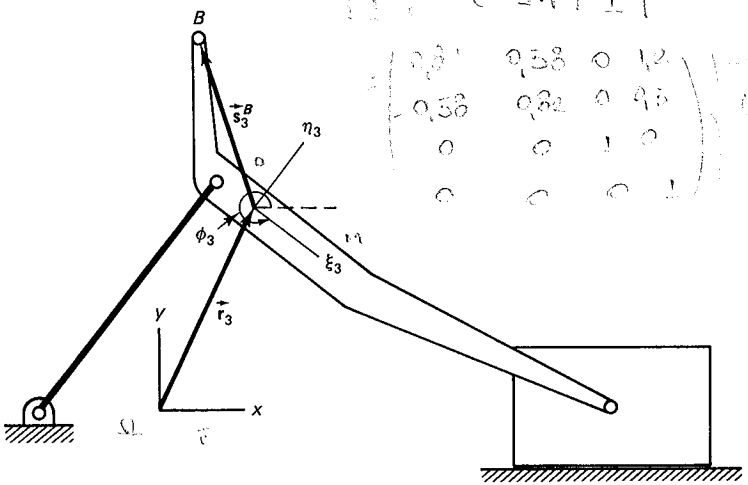

Solution The global components of $\vec{s}_3^B$ are found to be

$$\mathbf{s}_3^B = \mathbf{A}_3\mathbf{s}_3'^B = \begin{bmatrix} \cos\phi & -\sin\phi \\ \sin\phi & \cos\phi \end{bmatrix}_3 \begin{bmatrix} -1.8 \\ 1.3 \end{bmatrix} = \begin{bmatrix} -0.72 \\ 2.10 \end{bmatrix}$$

Hence the global coordinates of B are

$$\mathbf{r}_3^B = \mathbf{r}_3 + \mathbf{s}_3^B = \begin{bmatrix} 1.2 \\ 2.5 \end{bmatrix} + \begin{bmatrix} -0.72 \\ 2.10 \end{bmatrix} = \begin{bmatrix} 0.48 \\ 4.60 \end{bmatrix}$$

4.2 KINEMATIC CONSTRAINTS

In a mechanical system, the links and bodies may be interconnected by one or more kinematic joints. For example, the quick-return mechanism shown in Fig. 4.2(a) consists of five moving bodies interconnected by five revolute joints and two sliding joints. Since this mechanism undergoes planar motion, the motion of each moving body is described by three coordinates—two translational and one rotational. The kinematic joints in this system can be described as algebraic constraint equations.

In the following subsections, several commonly used kinematic joints are formulated. Some of these joints fall under the *lower-pair* category (LP) and the rest fall in the *higher-pair* (HP) category. The technique employed to formulate kinematic constraint equations for these joints may be applied to most other commonly used or special-purpose joints.

In general, formulation of lower-pair joints does not require any information on the shape (outline) of the connected bodies. For example, the quick-return mechanism of Fig. 4.2(a) can also be represented as shown in Fig. 4.2(b), where the body outlines are drawn arbitrarily. To derive constraint equations describing each joint, one need know only the position of the joint with respect to the bodies to which it is connected.

In some higher-pair joints, either the entire shape or a partial shape of the body outline must be known. For example, in analyzing the motion of a cam-follower pair, the full or partial outlines of the cam and the follower must be described. In some other higher-pair joints, instead of the shape of the outline, the shape or curvature of a slot on one of the bodies must be known.

In the following subsections, the constraint equations are denoted by $\mathbf{\Phi}$ with a superscript indicating the constraint type and the number of algebraic equations of that

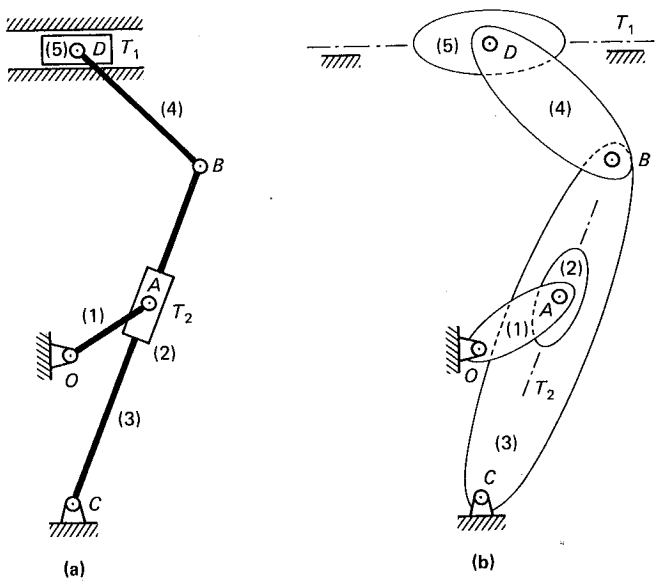

Figure 4.2 Quick-return mechanism: (a) schematic presentation and (b) its equivalent representation without showing the actual outlines.

expression. For example, $\mathbf{\Phi}^{(r,2)}$ denotes the *r*evolute joint constraint which contains two equations, and $\Phi^{(r\text{-}t,1)}$ denotes the *r*evolute-*t*ranslational joint constraint which contains one equation.

4.2.1 Revolute and Translational Joints (LP)

Revolute and translational joints are lower-pair kinematic joints. Examples of revolute joints are joints A, B, C, D, and O in the quick-return mechanism of Fig. 4.2. Schematic representation of a revolute joint connecting to bodies i and j is shown in Fig. 4.3. The center of the joint is denoted by point P. This point can be considered to be two coincident points; point P_i on body i and point P_j on body j. Location of point P on body i and body j can be described by the two vectors $\vec{s}_i^P$ and $\vec{s}_j^P$, where $\mathbf{s}'^P_i = [\xi^P, \eta^P]_i^T$ and $\mathbf{s}'^P_j = [\xi^P, \eta^P]_j^T$ are constants. The constraint equations for the revolute joint are obtained from the vector loop equation

$$\vec{r}_i + \vec{s}_i^P - \vec{s}_j^P - \vec{r}_j = \vec{0}$$

or

$$\mathbf{r}_i + \mathbf{s}_i^P - \mathbf{r}_j - \mathbf{s}_j^P = \mathbf{0}$$

which is equivalent to

$$\mathbf{\Phi}^{(r,2)} \equiv \mathbf{r}_i + \mathbf{A}_i\mathbf{s}'^P_i - \mathbf{r}_j - \mathbf{A}_j\mathbf{s}'^P_j = \mathbf{0} \tag{4.7}$$

More explicitly, Eq. 4.7 can be written in the form

$$\mathbf{\Phi}^{(r,2)} \equiv \begin{bmatrix} x_i^P - x_j^P \\ y_i^P - y_j^P \end{bmatrix} = \begin{bmatrix} 0 \\ 0 \end{bmatrix} \tag{4.8}$$

Equation 4.8 can be written in expanded form, using Eq. 4.3, as

$$\mathbf{\Phi}^{(r,2)} \equiv \begin{bmatrix} x_i + \xi_i^P \cos\phi_i - \eta_i^P \sin\phi_i - x_j - \xi_j^P \cos\phi_j + \eta_j^P \sin\phi_j \\ y_i + \xi_i^P \sin\phi_i + \eta_i^P \cos\phi_i - y_j - \xi_j^P \sin\phi_j - \eta_j^P \cos\phi_j \end{bmatrix} = \begin{bmatrix} 0 \\ 0 \end{bmatrix} \tag{4.9}$$

The two constraints of Eq. 4.7 reduce the number of degrees of freedom of the system by 2. Therefore, if the two bodies of Fig. 4.3 are not connected to any other bodies, then they have 4 degrees of freedom.

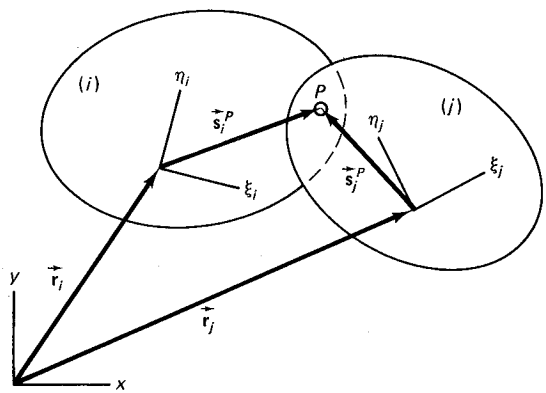

Figure 4.3 Revolute joint P connecting bodies i and j.

In the quick-return mechanism of Fig. 4.2, the two sliders (T_1 and T_2) are good examples of translational joints. This type of joint may appear in different shapes in a mechanism. Figure 4.4 illustrates several forms and presentations of translational joints. In a translational joint, the two bodies translate with respect to each other parallel to an axis known as the *line of translation;* therefore, there is no relative rotation between the bodies. For a translational joint, there are an infinite number of parallel lines of translation.

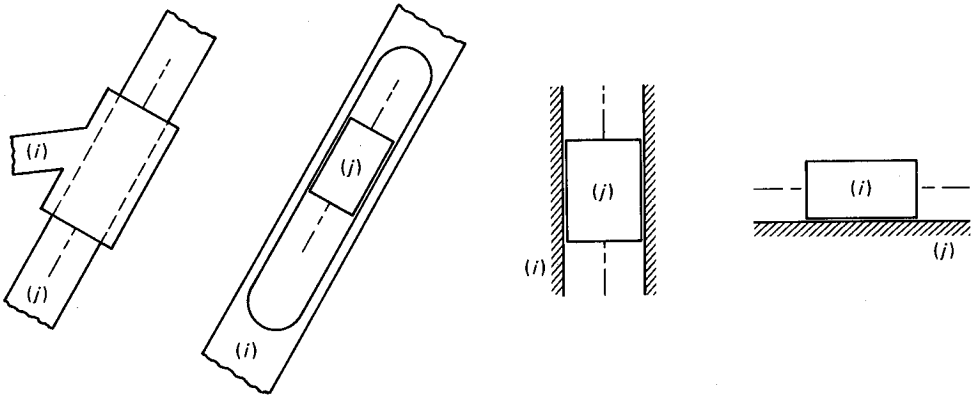

Figure 4.4 Different representations of a translational joint.

A constraint equation for eliminating the relative rotation between two bodies i and j is written as

$$\phi_i - \phi_j - (\phi_i^0 - \phi_j^0) = 0 \tag{4.10}$$

where ϕ_i^0 and ϕ_j^0 are the initial rotational angles. In order to eliminate the relative motion between the two bodies in a direction perpendicular to the line of translation, the two vectors $\vec{s}_i$ and $\vec{d}$ shown in Fig. 4.5 must remain parallel. These vectors are defined by locating three points on the line of translation—two points on body i and one point on body j. This condition is enforced by letting the vector product of these two vectors be

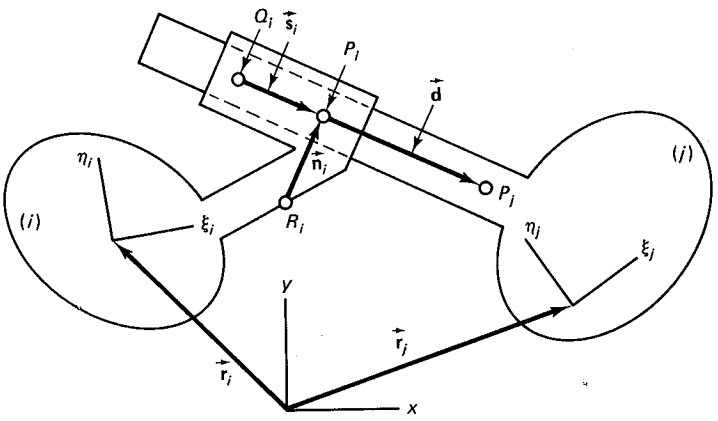

Figure 4.5 A translational joint between bodies i and j.

zero. A simple method would be to define another vector $\vec{n}_i$ perpendicular to the line of translation and to require that $\vec{d}$ remain perpendicular to $\vec{n}_i$; i.e., that

$$\mathbf{n}_i^T \mathbf{d} = 0$$

or

$$(x_i^P - x_i^R)(x_j^P - x_i^P) + (y_i^P - y_i^R)(y_j^P - y_i^P) = 0 \tag{4.11}$$

where

$$\mathbf{n}_i = \begin{bmatrix} x_i^P - x_i^R \\ y_i^P - y_i^R \end{bmatrix} \qquad \mathbf{d} = \begin{bmatrix} x_j^P - x_i^P \\ y_j^P - y_i^P \end{bmatrix}$$

If $n_i = s_i$, then

$$\mathbf{n}_i = \begin{bmatrix} x_i^P - x_i^R \\ y_i^P - y_i^R \end{bmatrix} = \begin{bmatrix} -(y_i^P - y_i^Q) \\ x_i^P - x_i^Q \end{bmatrix}$$

Therefore, Eqs. 4.10 and 4.11 yield the two constraint equations for a translational joint as†

$$\mathbf{\Phi}^{(t,2)} = \begin{bmatrix} (x_i^P - x_i^Q)(y_j^P - y_i^P) - (y_i^P - y_i^Q)(x_j^P - x_i^P) \\ \phi_i - \phi_j - (\phi_i^0 - \phi_j^0) \end{bmatrix} = \begin{bmatrix} 0 \\ 0 \end{bmatrix} \tag{4.12}$$

Note that a translational joint reduces the number of degrees of freedom of a system by 2.

Example 4.2

For the revolute and translational joints shown in the accompanying illustration, define the points needed in order to use Eqs. 4.9 and 4.12 and determine their coordinates.

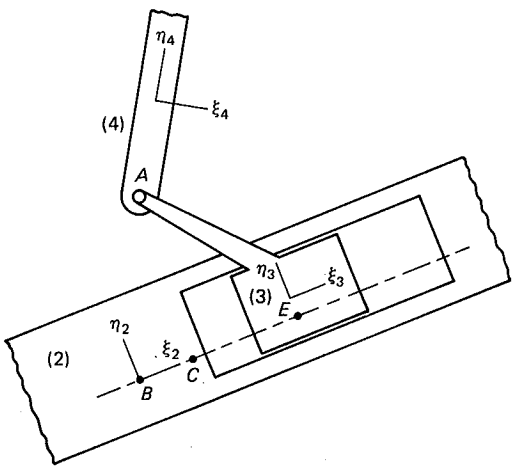

Solution The body-fixed coordinates of point A are

$$\xi_3^A = -1.6, \qquad \eta_3^A = 2.3, \qquad \xi_4^A = 0, \qquad \eta_4^A = -1.5$$

†The vector product of $\vec{s}_i$ and $\vec{d}$ gives directly the first constraint of Eq. 4.12.

These can be used for the revolute joint constraints of Eq. 4.9. For the translational joint, two points on body 2 and one point on body 3 are selected on a line parallel to the line of translation. The coordinates of these points are:

$$\xi_2^B = 0, \qquad \eta_2^B = 0, \qquad \xi_2^C = 1, \qquad \eta_2^C = 0, \qquad \xi_3^E = 0, \qquad \eta_3^E = -0.5$$

These coordinates can be used in the translational joint constraints of Eq. 4.11.

4.2.2 Composite Joints (LP)

The total number of constraint equations and coordinates describing a mechanical system can be reduced if some of the joints and bodies are combined into composite joints. This technique only simplifies the analytical formulation without changing the physical kinematic characteristics of the system. For example consider three bodies connected by two revolute joints, as shown schematically in Fig. 4.6(a). This system requires nine coordinates (three per body) and four constraint equations (two per revolute joint). Therefore, this system has $9 - 4 = 5$ degrees of freedom. This system may be represented by the kinematically equivalent system shown in Fig. 4.6(b). In this representation, body k and the two revolute joints are considered to be a *revolute-revolute* joint (rigid link) without any coordinates. This configuration requires six coordinates for bodies i and j, and as will be shown presently, one constraint equation for the revolute-revolute joint. Therefore, this equivalent system has $6 - 1 = 5$ degrees of freedom.

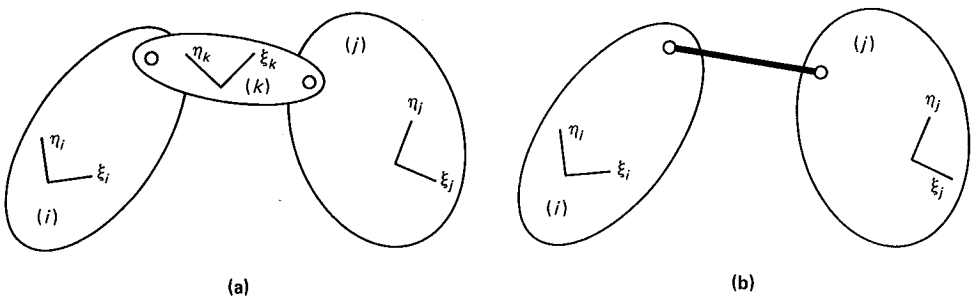

Figure 4.6 Two representations of the same system: (a) with three bodies and two revolute joints; (b) with two bodies and one revolute-revolute joint.

To formulate the constraint equation for a revolute-revolute joint, see Fig. 4.7, which illustrates two bodies connected by a link having length l. The length of the link is the distance between the centers of two revolute joints. The joint connectivity points on bodies i and j are shown as P_i and P_j. These points have fixed components $\mathbf{s}_i'^P$ and $\mathbf{s}_j'^P$ with respect to their corresponding body-fixed coordinate systems. The constraint equation can be derived by requiring that the magnitude of vector

$$\mathbf{d} = \mathbf{r}_j + \mathbf{s}_j^P - \mathbf{r}_i - \mathbf{s}_i^P = \begin{bmatrix} x_j^P - x_i^P \\ y_j^P - y_i^P \end{bmatrix}$$

connecting points P_i and P_j remain constant and equal to l. This constraint is written in the form

$$\Phi^{(r\text{-}r,1)} \equiv \mathbf{d}^T\mathbf{d} - l^2 = 0 \tag{4.13}$$

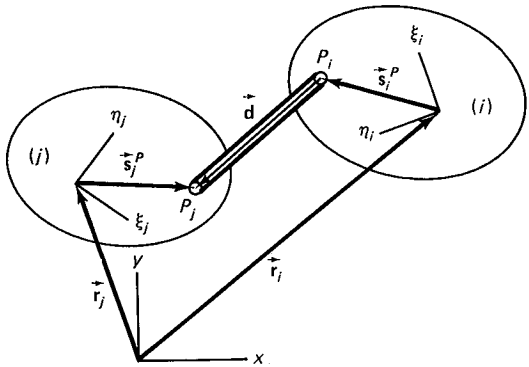

Figure 4.7 Revolute-revolute joint: a link connecting two bodies with two revolute joints.

Equation 4.13, if expanded, is written

$$\Phi^{(r\text{-}r,1)} \equiv (x_i^P - x_j^P)^2 + (y_i^P - y_j^P)^2 - l^2 = 0 \tag{4.14}$$

A second type of composite joint is called the *revolute-translational* joint. Figure 4.8 illustrates three examples of this type of joint. In Fig. 4.8(a), body i is connected to body k by a revolute joint and body k is connected to body j by a translational joint. The revolute joint, the translational joint, and body k can be combined into a composite joint in which point P on body i moves along an axis T on body j. Similar composite joints can be used in the mechanism of Fig. 4.8(b) by eliminating roller k as a body. The mechanism of Fig. 4.8(c) is identical in principle to the other two mechanisms; here, point P on body i moves on an axis parallel to the line of translation.

Figure 4.9 illustrates schematically a revolute-translational joint between bodies i and j. Point P_i on body i (the revolute joint) can move along the line of translation T (the translational joint) on body j. Two arbitrary points P_j and Q_j are chosen on the line of translation. A constraint equation for this joint is found by requiring two vectors $\vec{d}$ and $\vec{s}_j$ to remain parallel. Or, if a vector $\vec{n}_j$ is defined perpendicular to the line of translation, then

$$\mathbf{n}_j^T \mathbf{d} = 0 \tag{4.15}$$

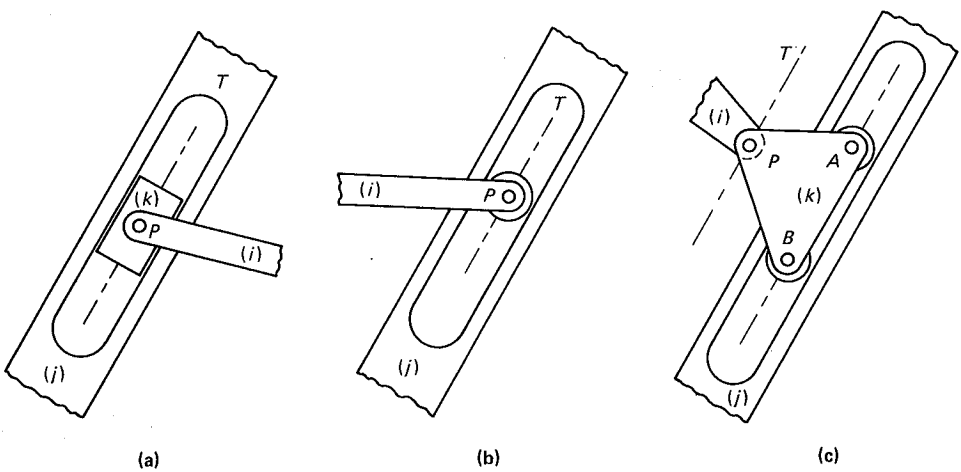

Figure 4.8 Examples of composite revolute-translational joints.

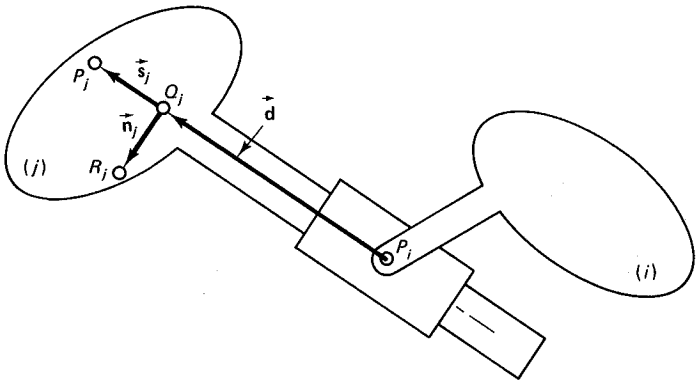

Figure 4.9 Revolute-translational joint configuration.

provides the same condition. If $s_j = n_j$, then

$$\mathbf{n}_j = \begin{bmatrix} x_j^R - x_j^Q \\ y_j^R - y_j^Q \end{bmatrix} = \begin{bmatrix} -(y_j^P - y_j^Q) \\ x_j^P - x_j^Q \end{bmatrix} \qquad \mathbf{d} = \begin{bmatrix} x_j^Q - x_i^P \\ y_j^Q - y_i^P \end{bmatrix}$$

and the constraint equation is written as

$$\Phi^{(t\text{-}r,\,1)} = (x_j^Q - x_i^P)(y_j^Q - y_j^P) - (y_j^Q - y_i^P)(x_j^Q - x_j^P) = 0 \tag{4.16}$$

Figure 4.10 shows an example of a mechanism with two revolute-translational joints. The slider and the revolute joint at point B can be combined to represent a revolute-translational joint. Similarly, the roller A and the revolute joint O can be combined and modeled as another revolute-translational joint.

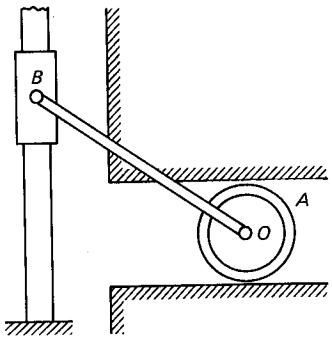

Figure 4.10 A mechanism with two revolute-translational joints.

4.2.3 Spur Gears and Rack and Pinion (HP)

Spur gears are used to transmit motion between parallel shafts. A pair of spur gears is shown in Fig. 4.11. The gears in Fig. 4.11(a) give the same motion to the shafts as the pair of equivalent rolling cylinders in Fig. 4.11(b). It is assumed that there is no slippage between the two cylinders.

The constraint formulation for a pair of spur gears as represented in Fig. 4.12(a) can be found easily. In this configuration the centers of the gears (shown here as circles)

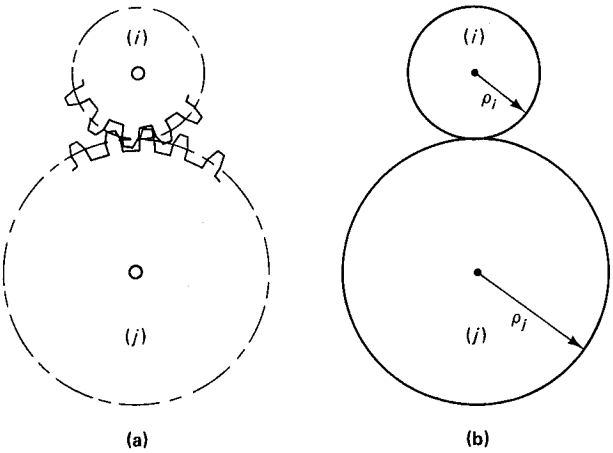

Figure 4.11 (a) A pair of spur gears, and (b) a pair of equivalent rolling cylinders.

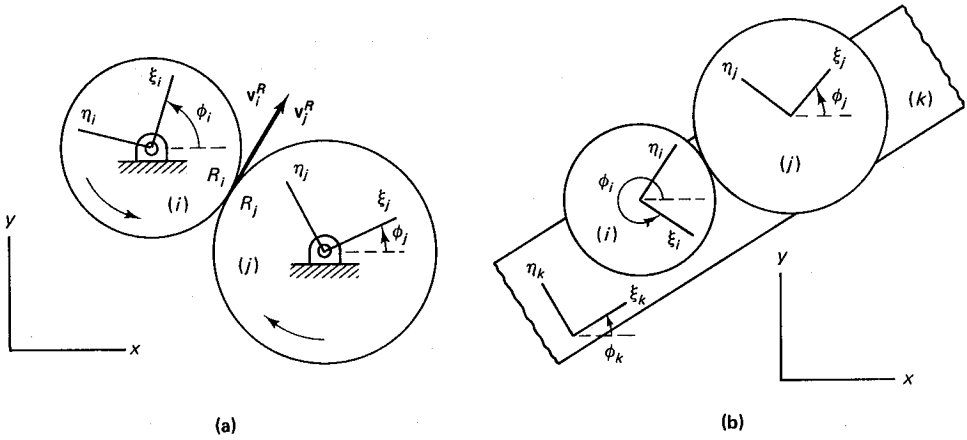

Figure 4.12 A pair of spur gears attached to (a) a nonmoving body and (b) a moving body.

do not move with respect to the xy coordinate system (ground or chassis). The points of contact R_i and R_j, at time t, have equal velocities; i.e.,

$$v_i^R = v_j^R \tag{a}$$

If body-fixed $\xi_i\eta_i$ and $\xi_j\eta_j$ coordinate systems are defined for each gear, then Eq. a can be written as

$$\rho_i\dot{\phi}_i = -\rho_j\dot{\phi}_j \tag{b}$$

Note that $\dot{\phi}_i$ and $\dot{\phi}_j$ always have opposite signs. Integrating Eq. b yields

$$\Phi^{(g-1,1)} \equiv (\phi_i - \phi_i^0)\rho_i + (\phi_j - \phi_j^0)\rho_j = 0 \tag{4.17}$$

where ϕ_i^0 and ϕ_j^0 are the initial conditions. Equation 4.17 is the constraint equation for a pair of spur gears with nonmoving centers. In this equation ϕ_i and ϕ_j must be assigned their accumulated angle of rotation; i.e., when bodies i and j rotate, the magnitudes of ϕ_i and ϕ_j may exceed $2\pi, 4\pi, \ldots$.

The constraint formulation for a pair of spur gears attached to a moving body k is shown in Fig. 4.12(b). Since all three bodies, i, j, and k, can rotate, the no-slippage condition at the contact point between bodies i and j can be written as

$$(\dot{\phi}_i - \dot{\phi}_k)\rho_i = -(\dot{\phi}_j - \dot{\phi}_k)\rho_j \tag{c}$$

Integrating Eq. c yields

$$\Phi^{(g\text{-}2,1)} \equiv [(\phi_i - \phi_i^0) - (\phi_k - \phi_k^0)]\rho_i + [(\phi_j - \phi_j^0) - (\phi_k - \phi_k^0)]\rho_j = 0 \tag{4.18}$$

If body k does not rotate, then $\phi_k = \phi_k^0$ and Eq. 4.18 becomes identical to Eq. 4.17.

In the constraint formulation of Eqs. 4.17 and 4.18, it is assumed that bodies i and j remain in contact. This condition is provided by the revolute joints connecting the gears to a third body. Therefore, there is only one relative degree of freedom between bodies i and j.

A rack and pinion can be considered a special form of a pair of spur gears in which the rack is a portion of a gear having an infinite pitch radius; thus its pitch circle is a straight line. A rack and pinion and its equivalent system, consisting of a rolling cylinder on a flat surface (a straight line), are shown in Fig. 4.13(a) and (b). It is assumed that no slippage occurs at the point of contact for the equivalent system.

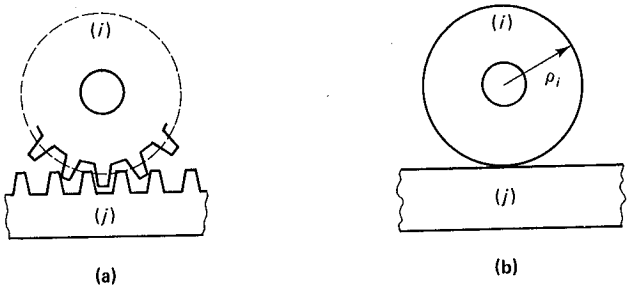

Figure 4.13 (a) A rack-and-pinion mechanism, and (b) the equivalent system.

Constraint formulation for a rack and pinion is derived for the two configurations in Fig. 4.14. The first configuration of a rack and pinion is shown in Fig. 4.14(a), where the pinion (body i) can rotate only with respect to the xy coordinate system and the rack can translate only parallel to the x axis. The condition for no slippage at the point of contact is written as

$$\dot{\phi}_i\rho_i = \dot{x}_j \tag{d}$$

Integrating Eq. d yields

$$\Phi^{(r\text{-}p\text{-}1,1)} \equiv (\phi_i - \phi_i^0)\rho_i - (x_j - x_j^0) = 0 \tag{4.19}$$

A second configuration of a rank-and-pinion mechanism is shown in Fig. 4.14(b), where the pinion can both rotate and translate parallel to the rack and the x axis. The no-slip condition is

$$\dot{x}_i + \dot{\phi}_i\rho_i = \dot{x}_j \tag{e}$$

Integrating Eq. e yields

$$\Phi^{(r\text{-}p\text{-}2,1)} \equiv (x_i - x_i^0) + (\phi_i - \phi_i^0)\rho_i - (x_j - x_j^0) = 0 \tag{4.20}$$

In the constraint formulation of Eqs. 4.19 and 4.20, it is assumed that bodies i and j remain in contact. This condition is provided by the revolute and translational joints

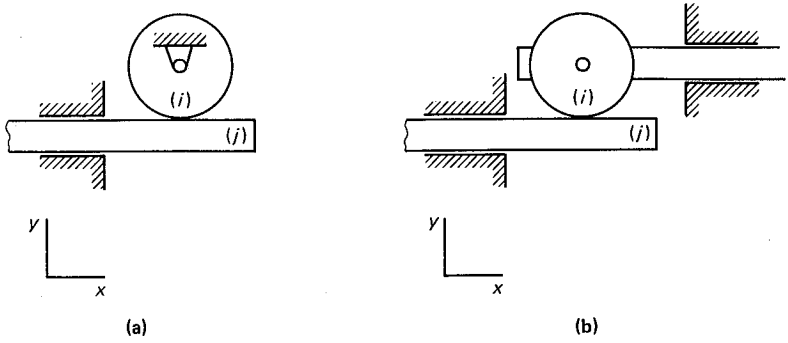

Figure 4.14 Rack-and-pinion mechanism in two different configurations.

connecting bodies i and j to a third body. Therefore, there is only one relative degree of freedom between bodies i and j.

In the configurations shown in Fig. 4.14, it is assumed that the line of translation remains parallel to the x axis. Constraint equations for the general case can also be derived where the third body can be in motion with respect to the xy coordinate system. Derivation of this constraint equation is left as an exercise for the reader.

4.2.4 Curve Representation

In some of the higher-pair joints, the shape of the outline of contacting bodies must be described analytically or numerically for kinematic analysis. If, for example, the outline of a cam is circular or elliptical, then it can be described analytically. However, in general, the outline must be described numerically.

Consider, as an example, the cam shown in Fig. 4.15(a). The outline of this cam can be discretized and described in polar coordinates at the points shown in Fig. 4.15(b). Angle θ is incremented counterclockwise from zero to 2π in equal or variable increments, and the corresponding values of s are recorded, as shown in Table 4.1. In order to describe this outline in a closed-form expression, a cubic interpolating *spline function* can be used.

A spline function is a function consisting of polynomial pieces on subintervals, joined together according to certain smoothness conditions. The choice of degree for the polynomial pieces most often made is 3. In this case, the resulting splines are termed *cubic splines*. The cubic polynomials are joined together in such a way that the resulting spline function has continuous first and second derivatives everywhere. For the curve segments shown in Fig. 4.16, if two cubic polynomials s_1 and s_2 are determined, then, the continuity conditions at point B, i.e., those for $\theta = \theta^B$, are

$$s_1 = s_2$$

$$\frac{ds_1}{d\theta} = \frac{ds_2}{d\theta}$$

$$\frac{d^2 s_1}{d\theta^2} = \frac{d^2 s_2}{d\theta^2}$$

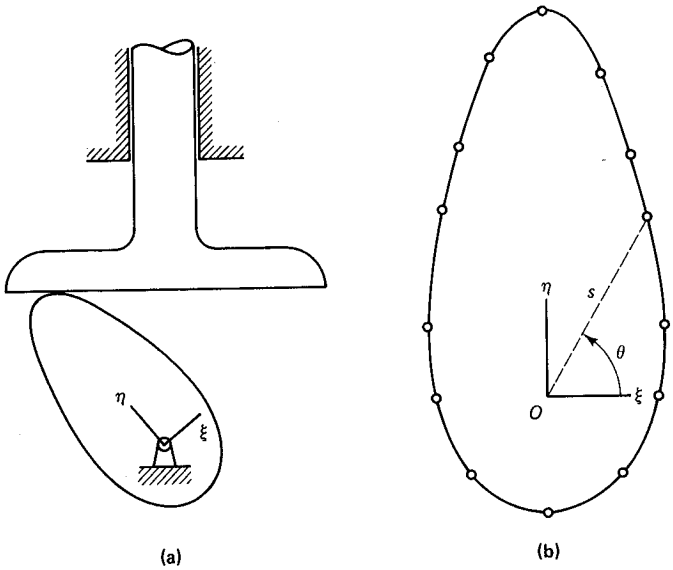

Figure 4.15 (a) A cam follower, and (b) discretization of the cam outline.

TABLE 4.1

Number	θ (deg)	s (cm)
1	0	3.70
2	30	4.55
3	60	6.80
4	70	8.38
5	80	10.65
6	90	12.46
7	100	11.10
8	110	8.65
9	120	7.04
10	150	4.63
11	180	3.80
12	225	3.62
13	270	3.80
14	315	3.62
15	360	3.70

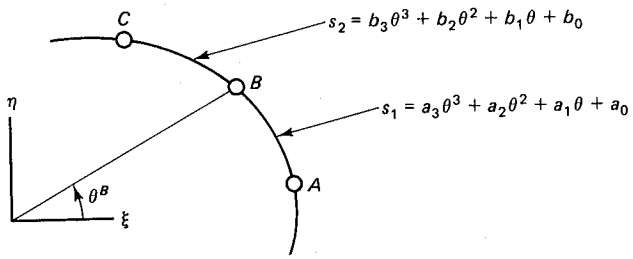

Figure 4.16 Two cubic polynomials describing segments of a curve.

A detailed discussion of cubic splines is outside the scope of this text. In most textbooks covering this subject, well-developed algorithms and computer programs are presented that can be applied to a discretized table of data, such as Table 4.1, to determine the corresponding cubic polynomials.

Example 4.3

The curve shown in the illustration is discretized and a portion of the recorded data is listed. A cubic spline function algorithm finds three cubic polynomials for

three segments of the curve as follows:

$$s_1 = -6.538\theta^3 + 3.230\theta^2 - 2.173\theta + 4.108$$
$$s_2 = 6.538\theta^3 - 8.538\theta^2 + 1.358\theta + 3.755$$
$$s_3 = -9.615\theta^3 + 10.846\theta^2 - 6.396\theta + 4.788$$

Show that s_1 and s_2 and their first and second derivatives are continuous at point B. Also, for a point P where $\theta^P = 0.26$ rad, find s, $ds/d\theta$, and $d^2s/d\theta^2$.

Point	θ (rad)	s (cm)
⋮	⋮	⋮
A	0.2	3.75
B	0.3	3.57
C	0.4	3.35
D	0.5	3.10
⋮	⋮	⋮

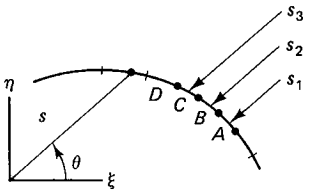

Solution At B, $\theta^B = 0.3$; therefore $s_1 = s_2 = 3.57$. The first derivatives of s_1 and s_2 are

$$\frac{ds_1}{d\theta} = -19.614\theta^2 + 6.460\theta - 2.173$$
$$\frac{ds_2}{d\theta} = 19.614\theta^2 - 17.076\theta + 1.358$$

Evaluating the first derivatives for $\theta = 0.3$ yields $ds_1/d\theta = ds_2/d\theta = -2.000$. The second derivatives of s_1 and s_2 are

$$\frac{d^2s_1}{d\theta^2} = -39.228\theta + 6.460$$
$$\frac{d^2s_2}{d\theta^2} = 39.228\theta - 17.076$$

Evaluating the second derivatives for $\theta = 0.3$ yields $d^2s_1/d\theta^2 = d^2s_2/d\theta^2 = -5.308$.

For point P, since $\theta^B \leqslant \theta^P \leqslant \theta^A$, function s_1 yields $s = 3.646$, $ds/d\theta = -1.819$, and $d^2s/d\theta^2 = -3.739$.

For any point on a curve, the $\xi\eta$ coordinates are found from the relations

$$\xi = s\cos\theta \qquad \eta = s\sin\theta \tag{4.21}$$

Then, the first and second derivatives of ξ and η with respect to θ are

$$\frac{d\xi}{d\theta} = -s\sin\theta + \frac{ds}{d\theta}\cos\theta \qquad \frac{d\eta}{d\theta} = s\cos\theta + \frac{ds}{d\theta}\sin\theta \tag{4.22}$$

and

$$\frac{d^2\xi}{d\theta^2} = -s\cos\theta - 2\frac{ds}{d\theta}\sin\theta + \frac{d^2s}{d\theta^2}\cos\theta$$
$$\frac{d^2\eta}{d\theta^2} = -s\sin\theta + 2\frac{ds}{d\theta}\cos\theta + \frac{d^2s}{d\theta^2}\sin\theta \tag{4.23}$$

For a point P, Eq. 4.22 represents the components of a vector tangent to the curve at P, as shown in Fig. 4.17, such as

$$\mathbf{g}'^P = \begin{bmatrix} \mu \\ \nu \end{bmatrix} \tag{4.24}$$

where $\mu = d\xi/d\theta$ and $\nu = d\eta/d\theta$.

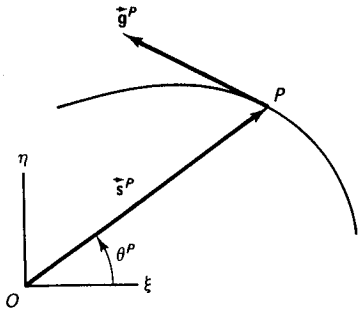

Figure 4.17 Vector tangent to a curve at point P.

Example 4.3a

Determine the $\xi\eta$ components of P, as defined at the beginning of Example 4.3, and then find the tangent vector $\vec{g}$ at P.

Solution Taking $\theta = 0.26$ and $s = 3.646$ and substituting into Eq. 4.21 yields $\xi^P = 3{,}523$ and $\eta^P = 0.937$. Since $ds/d\theta = -1.819$, then Eq. 4.22 yields $d\xi/d\theta = -2.695$ and $d\eta/d\theta = 3.056$; i.e., $\mathbf{g}'^P = [-2.695, 3.056]^T$.

The outline (or a portion of the outline) of a body can be expressed in polar coordinates with respect to a point different from the origin of the $\xi\eta$ axes. As shown in Fig. 4.18, the discretized portion of the outline is defined in terms of s and θ with respect to a point Q

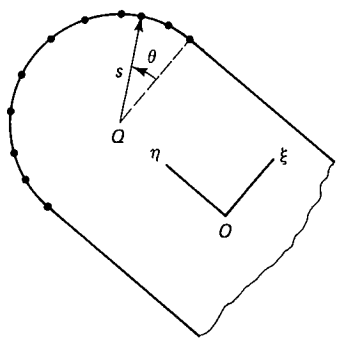

Figure 4.18 Polar coordinates of a point P with respect to point Q and the ξ axis.

and an axis parallel to the ξ axis. In this case, the ξ and η coordinates of any point on that portion of the outline are

$$\begin{aligned} \xi &= \xi^Q + s \cos \theta \\ \eta &= \eta^Q + s \sin \theta \end{aligned} \tag{4.25}$$

4.2.5 Cam-Followers (HP)

Cam-followers are used in a variety of designs; Fig. 4.19 shows a few of the many possible design variations. The contacting surfaces of a cam or a follower, in general, are

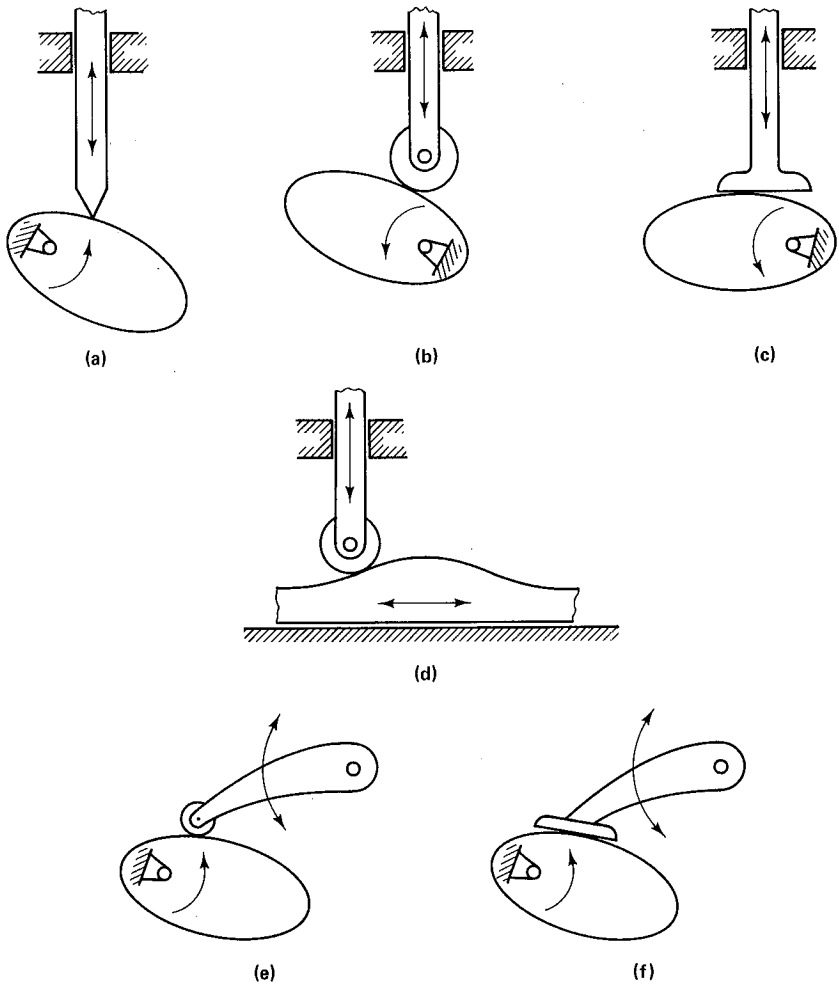

Figure 4.19 Several commonly used cam followers: (a) disk cam with offset point follower, (b) disk cam with radial roller follower, (c) disk cam with offset flat-faced follower, (d) translating cam with roller follower, (e) disk cam with oscillating roller follower, and (f) disk cam with oscillating flat-faced follower.

not expressible in closed-form functions. In this case, the cubic spline function method of Sec. 4.2.4 can be employed. In this section, the kinematic formulations for some of the cam-follower configurations are derived. It is assumed that the cam and the follower always remain in contact; i.e., no chattering is allowed.

The first formulation is derived for a disk cam with an offset point follower, as shown in Fig. 4.20. The cam is connected to a third body (possibly the chassis) with a revolute joint, and the follower is connected to this body with a translational joint. The third body may or may not move with respect to the global xy coordinate system. The coordinates of the contacting point P on body j (the follower) are known constant quantities $\mathbf{s}'^P_j = [\xi^P, \eta^P]^T_j$. The global coordinates of P_j are

$$\mathbf{r}^P_j = \mathbf{r}_j + \mathbf{A}_j \mathbf{s}'^P_j$$

The contacting point on body i (the cam) does not have constant coordinates; i.e., the elements of vector $\mathbf{s}'^P_i = [\xi^P, \eta^P]^T_i$ are functions of θ. The global coordinates of P_i are

$$\mathbf{r}^P_i = \mathbf{r}_i + \mathbf{A}_i \mathbf{s}'^P_i$$

Then, the constraint equations for this cam-follower pair can be written as

$$\mathbf{\Phi}^{(c\text{-}f\text{-}1,2)} \equiv \mathbf{r}^P_i - \mathbf{r}^P_j = \mathbf{0} \tag{4.26}$$

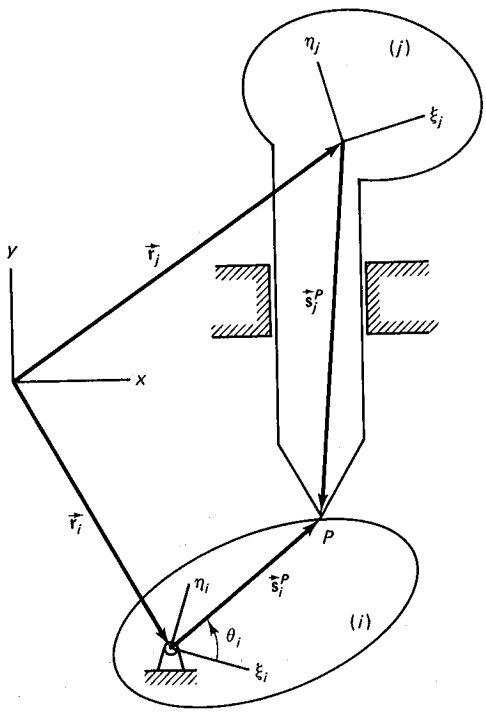

Figure 4.20 A disk cam and point-follower pair.

In expanded form, Eq. 4.26 is written

$$\begin{bmatrix} x \\ y \end{bmatrix}_i + \begin{bmatrix} \cos\phi & -\sin\phi \\ \sin\phi & \cos\phi \end{bmatrix}_i \begin{bmatrix} s\cos\theta \\ s\sin\theta \end{bmatrix}_i - \begin{bmatrix} x \\ y \end{bmatrix}_j - \begin{bmatrix} \cos\phi & -\sin\phi \\ \sin\phi & \cos\phi \end{bmatrix}_j \begin{bmatrix} \xi^P \\ \eta^P \end{bmatrix}_j = \begin{bmatrix} 0 \\ 0 \end{bmatrix} \tag{4.27}$$

Another type of cam-follower pair is the disk cam with offset roller follower shown in Fig. 4.21(a). The contact points P_i and P_j do not have known constant coordinates with respect to the bodies they are on. Vector $\vec{d}$ connecting point P_i to point Q_j is perpendicular to the tangent vector to either of the outlines at the contact point. The components of vector $\vec{d}$ can be found as follows:

$$\mathbf{d} = \mathbf{r}_j + \mathbf{A}_j \mathbf{s}'^Q_j - \mathbf{r}_i - \mathbf{A}_i \mathbf{s}'^P_i$$

Vector $\vec{d}$ is perpendicular to the tangent vector to the cam outline at P_i; therefore $\mathbf{g}_i^T\mathbf{d} = 0$. This condition alone does not eliminate the possibilities of penetration and separation shown in Fig. 4.21(b) and (c). If the magnitude of vector $\vec{d}$ is equal to the radius ρ of the roller, then there is no penetration or separation. This condition can be written as $\mathbf{d}^T\mathbf{d} - \rho^2 = 0$. Hence, there are two constraint equations for this pair:

$$\mathbf{\Phi}^{(c\text{-}f\text{-}2,2)} = \begin{bmatrix} \mathbf{g}_i^T\mathbf{d} \\ \mathbf{d}^T\mathbf{d} - \rho^2 \end{bmatrix} = \begin{bmatrix} 0 \\ 0 \end{bmatrix} \tag{4.28}$$

This formulation is also valid for the cam-follower of Fig. 4.19(e).

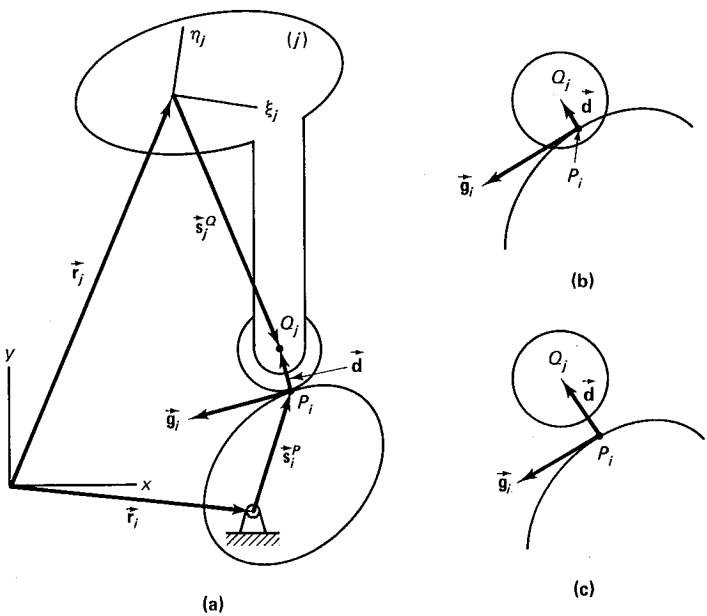

Figure 4.21 (a) Vector loop closure for a disk cam with follower pair, (b) penetration, and (c) separation of the outlines.

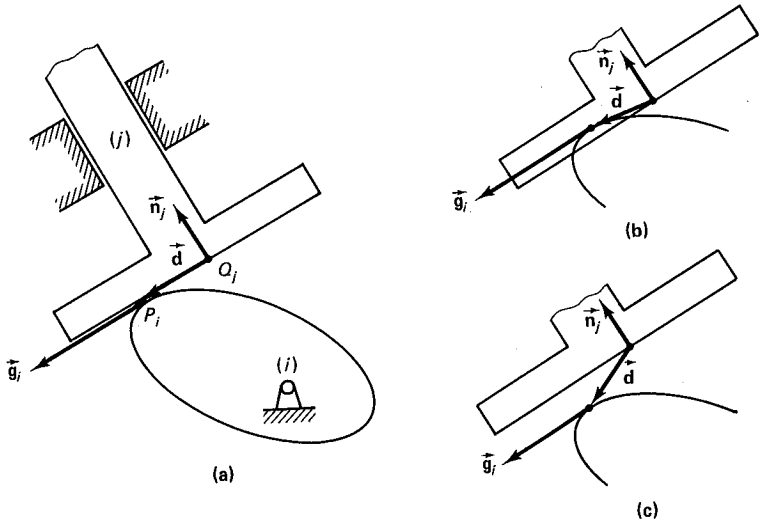

Figure 4.22 (a) A disk cam with an offset flat-faced follower, (b) penetration, and (c) separation of the outlines.

A disk cam with an offset flat-faced follower is shown in Fig. 4.22(a). A vector $\vec{n}_j$ is defined perpendicular to the contacting line (or face) of the follower, which must remain perpendicular to the tangent vector $\vec{g}_i$; i.e., $\mathbf{g}_i^T\mathbf{n}_j$ must be equal to 0. This condition alone does not eliminate the possibility of penetration or separation shown in Fig. 4.22(b) and (c). A vector connecting points P_i and Q_j is defined as $\mathbf{d} = \mathbf{r}_i^P - \mathbf{r}_j^Q$. This vector must also remain perpendicular to $\vec{n}_j$; i.e., $\mathbf{d}^T\mathbf{n}_j$ must be equal to 0. Therefore, the two constraint equations for this pair are

$$\mathbf{\Phi}^{(c\text{-}f\text{-}3,2)} = \begin{bmatrix} \mathbf{g}_i^T\mathbf{n}_j \\ \mathbf{d}^T\mathbf{n}_j \end{bmatrix} = \begin{bmatrix} 0 \\ 0 \end{bmatrix} \tag{4.29}$$

This formulation is also valid for the cam-follower of Fig. 4.19(f).

In the cam-follower formulation, θ is treated as an artificial coordinate. Hence, the vectors of coordinates for bodies i and j of a cam-follower pair are $\mathbf{q}_i = [x, y, \phi, \theta]_i^T$ and $\mathbf{q}_j = [x, y, \phi]_j^T$. It can be observed that for any of the cam-follower pairs shown in Fig. 4.19, there is one relative degree of freedom between the cam and its corresponding follower.

The constraint formulation has been derived in Eqs. 4.26, 4.28, and 4.29 for a general configuration applicable to various cam-follower mechanisms. For specific cases, the constraint formulation can be obtained in a much simpler form. The following example illustrates this point.

Example 4.4

Derive the constraint equation for the disk cam–follower shown in the illustration. The cam and the follower are attached to a nonmoving body. The motion of the follower is in the y direction, and the outline of the cam is circular.

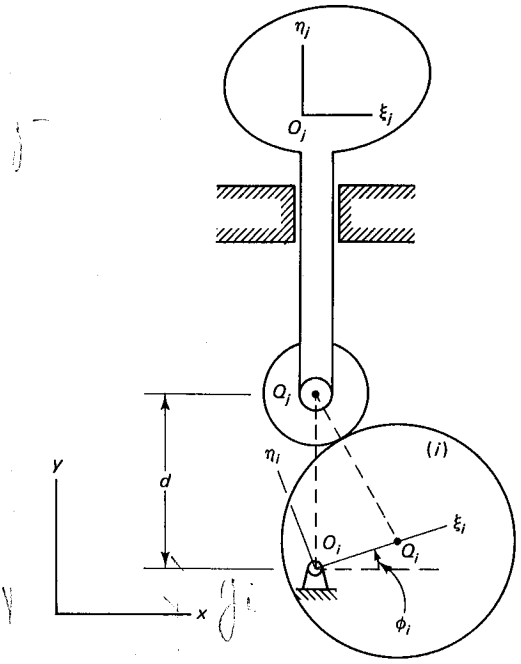

Solution If the radii of the cam and the roller are ρ_i and ρ_j, then a constraint equation can be written as

$$\Phi \equiv y_j - y_i + \eta_j^Q - d = 0 \qquad (a)$$

where d is expressed as a function of ϕ_i:

$$d \equiv (\rho_i + \rho_j) \cos \gamma + \xi_i^Q \sin \phi_i$$

The angle γ is found from the equation

$$\sin \gamma \equiv \frac{\xi_i^Q \cos \phi_i}{\rho_i + \rho_j}$$

It can be observed that for this special case, only one constraint equation is needed, and there is no need to introduce an artificial coordinate.

4.2.6 Point-Follower (HP)

Figure 4.23 shows part of a mechanism in which a slot is cut into one of the bodies. Pin A, which is rigidly attached to the other body, can slide in the slot. This type of kinematic higher pair is called a *point-follower* joint.

A point-follower joint between bodies i and j is shown schematically in Fig. 4.24. Pin P, which is attached to body i, can slide and rotate in a slot on body j. The coordinates of any point on the slot, relative to the body-fixed coordinate system on body j, can be described by Eq. 4.21; i.e., $\xi_j^P = s \cos \theta$ and $\eta_j^P = s \sin \theta$. The constraint equations for this joint are similar to the constraint equations of a revolute joint, with the exception that the position of point P on body j is not constant but varies as a function

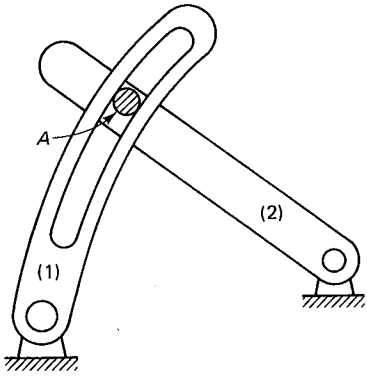

Figure 4.23 The motion relative to body 1 of point A attached to body 2 can be modeled by a point-follower joint.

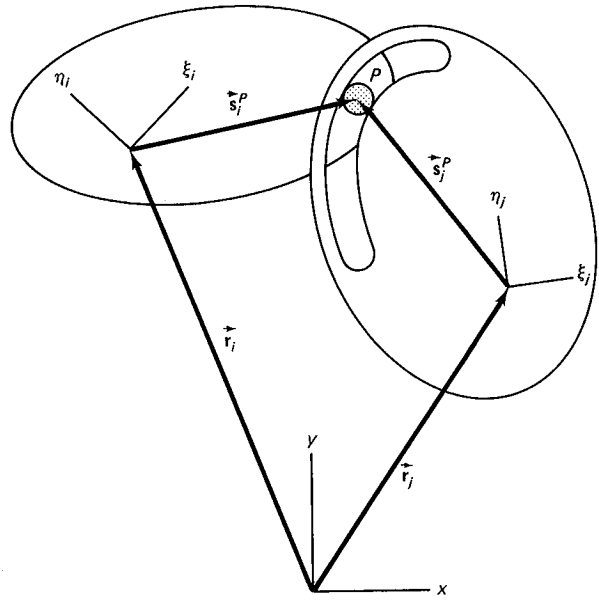

Figure 4.24 Point-follower joint: Pin P is attached rigidly to body i and can move in the slot embedded in body j.

of θ. Hence, the constraint equations are

$$\mathbf{\Phi}^{(p\text{-}f,2)} \equiv \begin{bmatrix} x_i^P - (x_j + \xi_j^P \cos\phi_j - \eta_j^P \sin\phi_j) \\ y_i^P - (y_j + \xi_j^P \sin\phi_j + \eta_j^P \cos\phi_j) \end{bmatrix} = \mathbf{0} \tag{4.30}$$

In this formulation θ is treated as an artificial coordinate and is added to the vector of coordinates, and both of the constraint equations of Eq. 4.30 are employed to describe the point-follower joint. This formulation does not provide any stopping condition when the pin reaches either end of the slot.

4.2.7 Simplified Constraints

The constraint equations describing certain kinematic conditions between two bodies can be simplified, in general, or replaced by other simple equations if one of the bodies is a nonmoving body; e.g., if one body is the chassis or ground. As an example, consider the quick-return mechanism shown in Fig. 4.25. Slider 3 is constrained to the ground with a translational joint and can move parallel to the y axis. Similarly, slider 4 is constrained to the ground with a translational joint and can move parallel to the x axis. The constraint equations of Eq. 4.12 can be used to formulate the kinematics of these two sliders. However, other equations can be used instead of Eq. 4.12. For example, slider 3 cannot move in the x direction or rotate; therefore, two equations of the form x_3 = constant and ϕ_3 = constant can be used. Similarly, since slider 4 cannot move in the y direction or rotate, y_4 = constant and ϕ_4 = constant can describe the translational con-

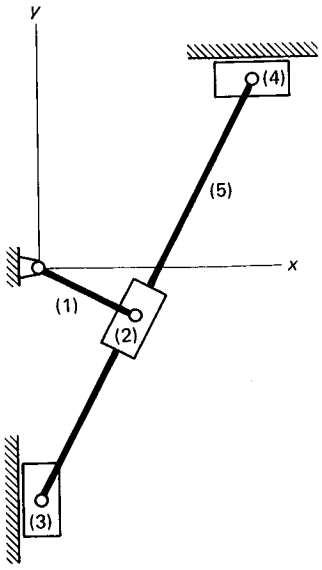

Figure 4.25 A quick-return mechanism.

straints for the slider. Therefore, in order to constrain translation of the origin or angular motion of a rigid body, one or more of the following equations may be used:

$$\Phi \equiv x_i - c_1 = 0 \tag{4.31}$$

$$\Phi \equiv y_i - c_2 = 0 \tag{4.32}$$

$$\Phi \equiv \phi_i - c_3 = 0 \tag{4.33}$$

where c_1, c_2, and c_3 are constant quantities. Figure 4.26 illustrates graphically the three constraints of Eqs. 4.31 through 4.33.

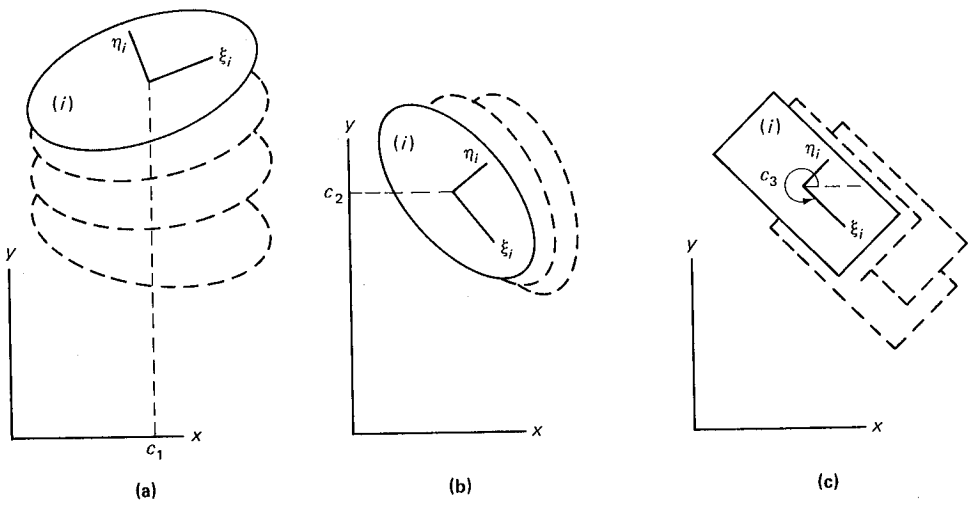

Figure 4.26 The body can move with (a) constant x_i, (b) constant y_i, and (c) constant ϕ_i.

To constrain the motion of point P_i on body i in the x or y direction, the following equations, which incorporate the results of Eq. 4.3, can be employed:

$$\begin{aligned}\Phi &\equiv x_i^P - c_4 \\ &= x_i + \xi_i^P \cos\phi_i - \eta_i^P \sin\phi_i - c_4 = 0 \end{aligned} \tag{4.34}$$

$$\begin{aligned}\Phi &\equiv y_i^P - c_5 \\ &= y_i + \xi_i^P \sin\phi_i + \eta_i^P \cos\phi_i - c_5 = 0 \end{aligned} \tag{4.35}$$

where c_4 and c_5 are constants.

4.2.8 Driving Links

In kinematically driven systems, the motion of one or more links (bodies) is usually defined. For example, in the quick-return mechanism of Fig. 4.27(a) or the slider-crank mechanism of Fig. 4.27(b), the *driving link i* rotates with known constant angular velocity ω. If kinematic analysis is to be performed using the appended driving constraints method of Sec. 3.2.2, then the motion of the driving link must be specified in the form of a driving constraint equation. For either of the mechanisms of Fig. 4.27, one moving constraint of the form

$$\Phi^{(d\text{-}1,1)} \equiv \phi_i - d_1(t) = 0 \tag{4.36}$$

can be employed, where $d_1(t) = \phi_i^0 + \omega t$ and ϕ_i^0 is the angle ϕ_i at $t = 0$. If the driving link rotates with a constant angular acceleration α, then Eq. 4.36 can be used with $d_1(t) = \frac{1}{2}\alpha t^2 + \dot{\phi}^0 t + \phi^0$, where $\dot{\phi}^0$ is the angular velocity at $t = 0$.

Equation 4.36 is not the only type of driving equation. Depending on the mechanism and the motion of its driving link(s), other forms of driving equation may be required. Some simple driving constraints are:

$$\Phi^{(d\text{-}2,1)} \equiv x_i - d_2(t) = 0 \tag{4.37}$$

$$\Phi^{(d\text{-}3,1)} \equiv y_i - d_3(t) = 0 \tag{4.38}$$

$$\Phi^{(d\text{-}4,1)} \equiv x_i^P - d_4(t) = 0 \tag{4.39}$$

$$\Phi^{(d\text{-}5,1)} \equiv y_i^P - d_5(t) = 0 \tag{4.40}$$

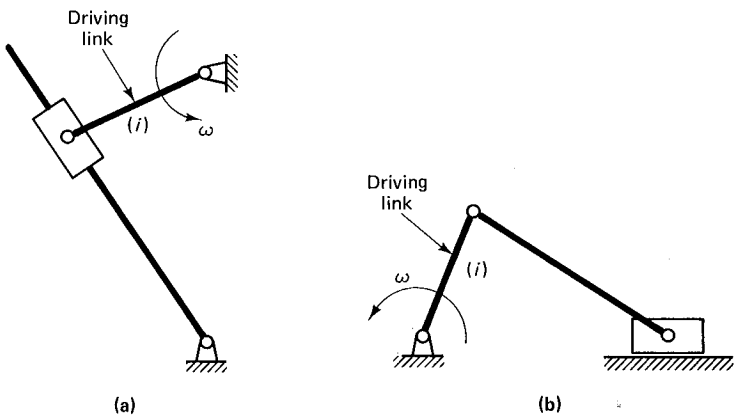

Figure 4.27 Driving link of (a) a quick-return mechanism and (b) a slider-crank mechanism.

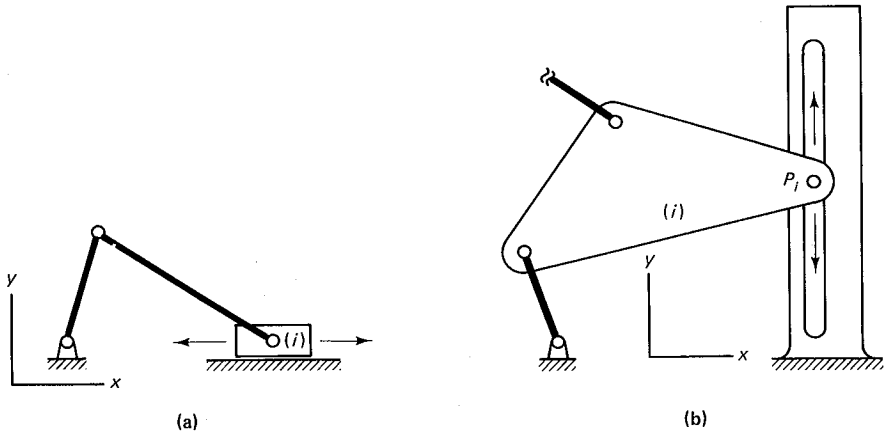

Figure 4.28 (a) The motion of the slider is controlled in the x direction, and (b) the motion of point P is controlled in the y direction.

For example, if the motion of the slider shown in Fig. 4.28(a) is controlled as a function of time, then Eq. 4.37 can be used as the driving constraint. For the mechanism of Fig. 4.28(b), the motion of point P in the y direction is controlled as a function of time; therefore, Eq. 4.40 can be employed as the driving constraint.

4.3 POSITION, VELOCITY, AND ACCELERATION ANALYSIS

The kinematic constraint equations $\mathbf{\Phi}$ derived in the preceding sections for planar kinematic pairs are, in general, nonlinear in terms of the coordinates $\mathbf{q}$. If the number of coordinates describing the configuration of a mechanical system is n and the number of degrees of freedom of the system is k, then $m = n - k$ kinematic constraints can be defined as

$$\mathbf{\Phi} \equiv \mathbf{\Phi}(\mathbf{q}) = \mathbf{0} \tag{4.41}$$

In addition, k driving constraint equations must be defined as

$$\mathbf{\Phi}^{(d)} \equiv \mathbf{\Phi}(\mathbf{q}, t) = \mathbf{0} \tag{4.42}$$

Equations 4.41 and 4.42 represent a set of n nonlinear algebraic equations which can be solved for n unknowns $\mathbf{q}$ at any given time $t = t^i$.

The procedure suggested here for solving Eqs. 4.41 and 4.42 is the appended driving constraint method of Sec. 3.2.2. These equations are identical in form to Eq. 3.12. The main difference between the formulation in this chapter and that in Chap. 3 is the dimension, i.e., the number of coordinates and, therefore, the number of constraint equations.

Example 4.5

A four-bar linkage was formulated for kinematic analysis in Example 3.2, using three coordinates, two kinematic constraint equations, and one driving constraint equation. Determine the number of coordinates and constraints if this mechanism is being analyzed using Cartesian coordinates.

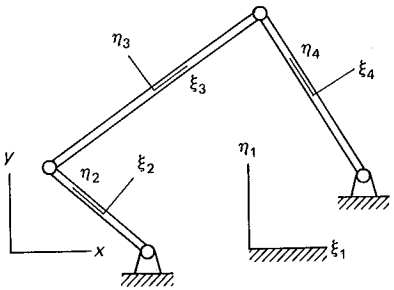

Solution Since there are four bodies in the system—three moving links and one stationary link—the dimension of $\mathbf{q}$ is $4 \times 3 = 12$. In the accompanying illustration, body-fixed coordinates are attached to each link. Body 1 is assumed to be the frame, and bodies 2, 3, and 4 are the crank, the coupler, and the follower, respectively. According to Eq. 4.7, each revolute joint is represented by two algebraic equations, and therefore there are $4 \times 2 = 8$ algebraic equations representing all four revolute joints. In addition, since body 1 does not move with respect to the xy coordinate system, three simple constraints in the form of Eqs. 4.31 through 4.33 are needed. Therefore, the total number of kinematic constraints is $m = 8 + 3 = 11$. For the rotation of the crank, one driving constraint makes the total number of equations equal to 12.

The first and second time derivatives of Eqs. 4.41 and 4.42 yield velocity and acceleration equations that are identical in form to Eqs. 3.13 and 3.15. For position analysis using the Newton-Raphson algorithm, velocity analysis, and acceleration analysis, the Jacobian matrix of the kinematic constraints, $\mathbf{\Phi}_\mathbf{q}$, is needed. Also, for acceleration analysis, the right side of the kinematic acceleration equations, vector $\boldsymbol{\gamma}$ as given in Eq. 3.17, is needed. For each of the kinematic pairs discussed in the preceding sections closed-form expressions can be derived for the entries of the Jacobian matrix and the right-side vector of the acceleration equations. From these expressions plus the constraint equations, all of the necessary terms for kinematic analysis can be assembled systematically. In Sec. 4.3.1, these expressions are derived in detail for some of the kinematic pairs. The method can be applied similarly to other constraint equations.

Derivation of the velocity and acceleration equations requires the time derivatives of the constraint equations. In turn, these require the derivatives of the coordinates of the points describing the kinematic joint. The xy coordinates of a point P attached to body i can be found from Eq. 4.1, where it is assumed that the position of the point on the body and the coordinates of the body are known. The velocity of the point in the xy coordinate system can be found by taking the time derivative of Eq. 4.1,

$$\begin{aligned}\dot{\mathbf{r}}_i^P &= \dot{\mathbf{r}}_i + \dot{\mathbf{A}}_i \mathbf{s}_i'^P \\ &= \dot{\mathbf{r}}_i + \mathbf{B}_i \mathbf{s}_i'^P \dot{\phi}_i\end{aligned} \tag{4.43}$$

where

$$\mathbf{B}_i = \begin{bmatrix} -\sin\phi & -\cos\phi \\ \cos\phi & -\sin\phi \end{bmatrix}_i \tag{4.44}$$

Similarly, the time derivative of Eq. 4.43 yields the acceleration of point P:

$$\begin{aligned}\ddot{\mathbf{r}}_i^P &= \ddot{\mathbf{r}}_i + \ddot{\mathbf{A}}_i \mathbf{s}_i'^P \\ &= \ddot{\mathbf{r}}_i + \mathbf{B}_i \mathbf{s}_i'^P \ddot{\phi}_i - \mathbf{A}_i \mathbf{s}_i'^P \dot{\phi}_i^2 \end{aligned} \tag{4.45}$$

Knowing the velocity of body i, i.e., $\dot{\mathbf{q}}_i = [\dot{\mathbf{r}}^T, \dot{\phi}]_i^T$, we can use Eq. 4.43 to find the velocity of P_i; and similarly, knowing the velocity and the acceleration of body i; i.e., $\dot{\mathbf{q}}_i$ and $\ddot{\mathbf{q}}_i$, we can find the acceleration of P_i by using Eq. 4.45.

4.3.1 Systematic Generation of Some Basic Elements

Systematic generation of the Jacobian matrix and the right side of the acceleration equations for some of the standard kinematic joints can best be illustrated by deriving these elements for a revolute joint.

Consider the revolute-joint constraint equations of Sec. 4.2.1. These equations in compact form are written as

$$\mathbf{\Phi}^{(r,2)} \equiv \mathbf{r}_i + \mathbf{A}_i \mathbf{s}_i'^P - \mathbf{r}_j - \mathbf{A}_j \mathbf{s}_j'^P = \mathbf{0}$$

and in expanded form they are

$$\Phi^{(r,\,1\text{st})} \equiv x_i + \xi_i^P \cos\phi_i - \eta_i^P \sin\phi_i - x_j - \xi_j^P \cos\phi_j + \eta_j^P \sin\phi_j = 0$$

$$\Phi^{(r,\,2\text{nd})} \equiv y_i + \xi_i^P \sin\phi_i + \eta_i^P \cos\phi_i - y_j - \xi_j^P \sin\phi_j - \eta_j^P \cos\phi_j = 0$$

The partial derivative of these equations with respect to $\mathbf{q}$, i.e., $\mathbf{\Phi}_{\mathbf{q}}^{(r,2)}$, provides two rows to the overall system Jacobian. Since $\mathbf{\Phi}^{(r,2)}$ is a function of only $\mathbf{q}_i$ and $\mathbf{q}_j$, $\mathbf{\Phi}_{\mathbf{q}}^{(r,2)}$ may have nonzero elements only in the columns associated with $\mathbf{q}_i$ and $\mathbf{q}_j$. These possible nonzero entries are

$$\begin{aligned}
1 \equiv \frac{\partial \Phi^{(r,\,1\text{st})}}{\partial x_i} &= 1.0 \\
\frac{\partial \Phi^{(r,\,1\text{st})}}{\partial y_i} &= 0.0 \\
2 \equiv \frac{\partial \Phi^{(r,\,1\text{st})}}{\partial \phi_i} &= -\xi_i^P \sin\phi_i \overset{-}{\oplus} \eta_i^P \cos\phi_i \\
&= -y_i^P + y_i \\
3 \equiv \frac{\partial \Phi^{(r,\,1\text{st})}}{\partial x_j} &= -1.0 \\
\frac{\partial \Phi^{(r,\,1\text{st})}}{\partial y_j} &= 0.0 \\
4 \equiv \frac{\partial \Phi^{(r,\,1\text{st})}}{\partial \phi_j} &= \xi_j^P \sin\phi_j + \eta_j^P \cos\phi_j \\
&= y_j^P - y_j \\
\frac{\partial \Phi^{(r,\,2\text{nd})}}{\partial x_i} &= 0.0
\end{aligned} \tag{4.46}$$

$$
\begin{aligned}
(5) &\equiv \frac{\partial \Phi^{(r,\,2\text{nd})}}{\partial y_i} = 1.0 \\
(6) &\equiv \frac{\partial \Phi^{(r,\,2\text{nd})}}{\partial \phi_i} = \xi_i^P \cos\phi_i - \eta_i^P \sin\phi_i \\
&\qquad\qquad\qquad\quad = x_i^P - x_i \\
&\frac{\partial \Phi^{(r,\,2\text{nd})}}{\partial x_j} = 0.0 \\
(7) &\equiv \frac{\partial \Phi^{(r,\,2\text{nd})}}{\partial y_j} = -1.0 \\
(8) &\equiv \frac{\partial \Phi^{(r,\,2\text{nd})}}{\partial \phi_j} = -\xi_j^P \cos\phi_j + \eta_j^P \sin\phi_j \\
&\qquad\qquad\qquad\quad = -x_j^P + x_j
\end{aligned}
$$

where four of the entries are identically zero. The position of these nonzero entries† in the rows of the Jacobian matrix corresponding to $\mathbf{\Phi}^{(r,2)}$ and columns corresponding to $\mathbf{q}_i$ and $\mathbf{q}_j$ is shown in Fig. 4.29.

$$
\begin{array}{l}
\\
\partial\Phi^{(r,\,1\text{st})}/\partial\ldots \\
\partial\Phi^{(r,\,2\text{nd})}/\partial\ldots
\end{array}
\begin{array}{c}
\begin{array}{cccccc} x_i & y_i & \phi_i & x_j & y_j & \phi_j \end{array} \\
\begin{bmatrix} (1) & 0 & (2) & (3) & 0 & (4) \\ 0 & (5) & (6) & 0 & (7) & (8) \end{bmatrix}
\end{array}
$$

Figure 4.29 Nonzero entities of the Jacobian matrix for a revolute joint between bodies i and j.

The entries of the Jacobian matrix can also be found by taking the time derivative of the constraint equations. The time derivative of the constraint equations for a revolute joint is

$$
\begin{aligned}
\dot{x}_i - (\xi_i^P \sin\phi_i + \eta_i^P \cos\phi_i)\dot{\phi}_i - \dot{x}_j + (\xi_j^P \sin\phi_j + \eta_j^P \cos\phi_j)\dot{\phi}_j &= 0 \\
\dot{y}_i + (\xi_i^P \cos\phi_i - \eta_i^P \sin\phi_i)\dot{\phi}_i - \dot{y}_j - (\xi_j^P \cos\phi_j - \eta_j^P \sin\phi_j)\dot{\phi}_j &= 0
\end{aligned}
$$

or

$$
\begin{bmatrix} (1) & 0 & (2) & (3) & 0 & (4) \\ 0 & (5) & (6) & 0 & (7) & (8) \end{bmatrix}
\begin{bmatrix} \dot{x}_i \\ \dot{y}_i \\ \dot{\phi}_i \\ \dot{x}_j \\ \dot{y}_j \\ \dot{\phi}_j \end{bmatrix}
= \begin{bmatrix} 0 \\ 0 \end{bmatrix}
$$

This velocity equation is in the same form shown by the first equation of Eq. 3.13.

To obtain the right side of the acceleration equation for a revolute joint, either Eq. 3.17 can be used with the Jacobian matrix of Eq. 4.46, or the velocity equations can

†In this text, the term *nonzero entry* must be interpreted as an entry with a possible nonzero value.

be differentiated with respect to time to obtain the acceleration equations:

$$\ddot{x}_i - (\xi_i^P \sin\phi_i + \eta_i^P \cos\phi_i)\ddot{\phi}_i - (\xi_i^P \cos\phi_i - \eta_i^P \sin\phi_i)\dot{\phi}_i^2 - \ddot{x}_j$$
$$+ (\xi_j^P \sin\phi_j + \eta_j^P \cos\phi_j)\ddot{\phi}_j + (\xi_j^P \cos\phi_j - \eta_j^P \sin\phi_j)\dot{\phi}_j^2 = 0$$

$$\ddot{y}_i + (\xi_i^P \cos\phi_i - \eta_i^P \sin\phi_i)\ddot{\phi}_i - (\xi_i^P \sin\phi_i + \eta_i^P \cos\phi_i)\dot{\phi}_i^2 - \ddot{y}_j$$
$$- (\xi_j^P \cos\phi_j - \eta_j^P \sin\phi_j)\ddot{\phi}_j + (\xi_j^P \sin\phi_j + \eta_j^P \cos\phi_j)\dot{\phi}_j^2 = 0$$

or

$$\begin{bmatrix} 1 & 0 & 2 & 3 & 0 & 4 \\ 0 & 5 & 6 & 0 & 7 & 8 \end{bmatrix} \begin{bmatrix} \ddot{x}_i \\ \ddot{y}_i \\ \ddot{\phi}_i \\ \ddot{x}_j \\ \ddot{y}_j \\ \ddot{\phi}_j \end{bmatrix} = \boldsymbol{\gamma}^{(r,2)}$$

where

$$\boldsymbol{\gamma}^{(r,2)} = \begin{bmatrix} (\xi_i^P \cos\phi_i - \eta_i^P \sin\phi_i)\dot{\phi}_i^2 - (\xi_j^P \cos\phi_j - \eta_j^P \sin\phi_j)\dot{\phi}_j^2 \\ (\xi_i^P \sin\phi_i + \eta_i^P \cos\phi_i)\dot{\phi}_i^2 - (\xi_j^P \sin\phi_j + \eta_j^P \cos\phi_j)\dot{\phi}_i^2 \end{bmatrix}$$
$$= \begin{bmatrix} (x_i^P - x_i)\dot{\phi}_i^2 - (x_j^P - x_j)\dot{\phi}_j^2 \\ (y_i^P - y_i)\dot{\phi}_i^2 - (y_j^P - y_j)\dot{\phi}_j^2 \end{bmatrix}$$
$$= \mathbf{s}_i^P \dot{\phi}_i^2 - \mathbf{s}_j^P \dot{\phi}_j^2 \tag{4.47}$$

From Eqs. 4.46 and 4.47, it can be observed that the entries of the Jacobian matrix and the vector of the right side of the acceleration equations for a revolute joint can be generated systematically, in a computer program.

Tables 4.2 and 4.3 summarize the elements of the Jacobian matrix and the vector $\boldsymbol{\gamma}$, respectively, for some of the constraint equations of the basic joints. Similar elements can be derived for other kinematic pairs. Verification of these elements is left as an exercise for the reader.

4.4 KINEMATIC MODELING

In general, there are many ways to kinematically model a particular mechanism, any one of which may be more advantageous in some circumstances. In kinematic analysis, the problem size, i.e., the number of coordinates and number of constraint equations, is an important factor to consider. A small number of coordinates yields a smaller problem to solve. In this section, several simple examples are considered to illustrate methods of kinematic modeling. The same techniques may be used to analyze larger problems.

4.4.1 Slider-Crank Mechanism

The *slider-crank* is one of the most widely used mechanisms in practice. This mechanism finds its greatest application in the internal-combustion engine. The mechanism is

TABLE 4.2 Elements of the Jacobian Matrix for Some of the Basic Constraint Equations

	$\partial\Phi/\partial x_i$	$\partial\Phi/\partial y_i$	$\partial\Phi/\partial \phi_i$	$\partial\Phi/\partial x_j$	$\partial\Phi/\partial y_j$	$\partial\Phi/\partial \phi_j$
$\Phi^{(r,2)}$	1	0	$-(y_i^P - y_i)$	-1	0	$(y_j^P - y_j)$
	0	1	$(x_i^P - x_i)$	0	-1	$-(x_j^P - x_j)$
$\Phi^{(t,2)}$	$(y_i^P - y_i^Q)$	$-(x_i^P - x_i^Q)$	$-(x_j^P - x_i)(x_i^P - x_i^Q) - (y_j^P - y_i)(y_i^P - y_i^Q)$	$-(y_i^P - y_i^Q)$	$(x_i^P - x_i^Q)$	$(x_j^P - x_j)(x_i^P - x_i^Q) + (y_j^P - y_j)(y_i^P - y_i^Q)$
	0	0	1	0	0	-1
$\Phi^{(r-r,1)}$	$2(x_i^P - x_j^P)$	$2(y_i^P - y_j^P)$	$-2(x_i^P - x_j^P)(y_i^P - y_i) + 2(y_i^P - y_j^P)(x_i^P - x_i)$	$-2(x_i^P - x_j^P)$	$-2(y_i^P - y_j^P)$	$2(x_i^P - x_j^P)(y_j^P - y_j) - 2(y_i^P - y_j^P)(x_j^P - x_j)$
$\Phi^{(r-t,1)}$	$(y_j^P - y_j^Q)$	$-(x_j^P - x_j^Q)$	$-(y_i^P - y_i)(y_j^P - y_j^Q) - (x_i^P - x_i)(x_j^P - x_j^Q)$	$-(y_j^P - y_j^Q)$	$(x_j^P - x_j^Q)$	$(y_i^P - y_j)(y_j^P - y_j^Q) + (x_i^P - x_j)(x_j^P - x_j^Q)$

TABLE 4.3 Vector γ for Some of the Basic Constraint Equations

	γ
$\Phi^{(r,2)}$	$(x_i^P - x_i)\dot{\phi}_i^2 - (x_j^P - x_j)\dot{\phi}_j^2$
	$(y_i^P - y_i)\dot{\phi}_i^2 - (y_j^P - y_j)\dot{\phi}_j^2$
$\Phi^{(t,2)}$	$-2[(x_i^P - x_i^Q)(\dot{x}_i - \dot{x}_j) + (y_i^P - y_i^Q)(\dot{y}_i - \dot{y}_j)]\dot{\phi}_i$† $- [(x_i^P - x_i^Q)(y_i - y_j) - (y_i^P - y_i^Q)(x_i - x_j)]\dot{\phi}_i^2$
	0
$\Phi^{(r-r,1)}$	$-2\{(\dot{x}_i - \dot{x}_j)^2 + (\dot{y}_i - \dot{y}_j)^2$ $+ [(x_i^P - x_i)(x_j^P - x_i) + (y_i^P - y_i)(y_j^P - y_i)]\dot{\phi}_i^2$ $+ [(x_j^P - x_j)(x_i^P - x_j) + (y_j^P - y_j)(y_i^P - y_j)]\dot{\phi}_j^2$ $- 2[(x_i^P - x_i)(x_j^P - x_j) + (y_i^P - y_i)(y_j^P - y_j)]\dot{\phi}_i\dot{\phi}_j$ $+ 2[(x_i^P - x_i)(\dot{y}_i - \dot{y}_j) - (y_i^P - y_i)(\dot{x}_i - \dot{x}_j)]\dot{\phi}_i$ $- 2[(x_j^P - x_j)(\dot{y}_i - \dot{y}_j) - (y_j^P - y_j)(\dot{x}_i - \dot{x}_j)]\dot{\phi}_j\}$
$\Phi^{(r-t,1)}$	$[(x_i^P - x_i)(y_j^P - y_j^Q) - (y_i^P - y_i)(x_j^P - x_j^Q)(\dot{\phi}_i - 2\dot{\phi}_j)\dot{\phi}_i$ $+ [(x_i^P - x_j)(y_j^P - y_j^Q) - (y_i^P - y_j)(x_j^P - x_j^Q)]\dot{\phi}_j^2$ $- 2[(x_j^P - x_j^Q)(\dot{x}_i - \dot{x}_j) + (y_j^P - y_j^Q)(\dot{y}_i - \dot{y}_j)]\dot{\phi}_j$

†Note that $\dot{\phi}_i = \dot{\phi}_j$.

made of four links or bodies, as illustrated in Fig. 4.30(a). The bodies are numbered from 1 to 4, as shown in Fig. 4.30(b). Body 1 is the fixed link (ground, chassis, or engine block), body 2 is the crank, body 3 is the connecting rod, and body 4 is the slider. Bodies 1 and 2, 2 and 3, and 3 and 4 are connected by revolute joints A, B, and O, respectively. Bodies 1 and 4 are connected by a translational joint T. The number of degrees of freedom for this mechanism is $k = 4 \times 3 - (3 \times 2 + 1 \times 2 + 3) = 1$, since there are $4 \times 3 = 12$ coordinates in the system, 3 revolute joints eliminate 6 DOF, 1 translational joint eliminates 2 DOF, and ground constraints on body 1 eliminate 3 DOF.

Body-fixed coordinates $\xi\eta$ are attached to each body, including the ground, as shown in Fig. 4.30(c). Positioning of these coordinate systems is quite arbitrary for kinematic analysis. However, it is good practice to locate the origin of the coordinate system at the center of gravity of the body. Furthermore, aligning at least one of the coordinate axes with the link axis or parallel to some line of certain geometric or kinematic importance may simplify the task of collecting data for the kinematic pairs in the system.

For the three revolute joints, the following data are obtained from Fig. 4.30(c):

$$\begin{aligned} &\xi_4^A = 0.0, && \eta_4^A = 0.0, && \xi_3^A = -200.0, && \eta_3^A = 0.0 \\ &\xi_3^B = 300.0, && \eta_3^B = 0.0, && \xi_2^B = -100.0, && \eta_2^B = 0.0 \\ &\xi_2^0 = 100.0 && \eta_2^0 = 0.0, && \xi_1^0 = 0.0, && \eta_1^0 = 0.0 \end{aligned} \qquad (a)$$

For the translational joint, two points on body 4 and one point on body 1 are chosen. The location of these points is arbitrary, as long as they are on the same line of transla-

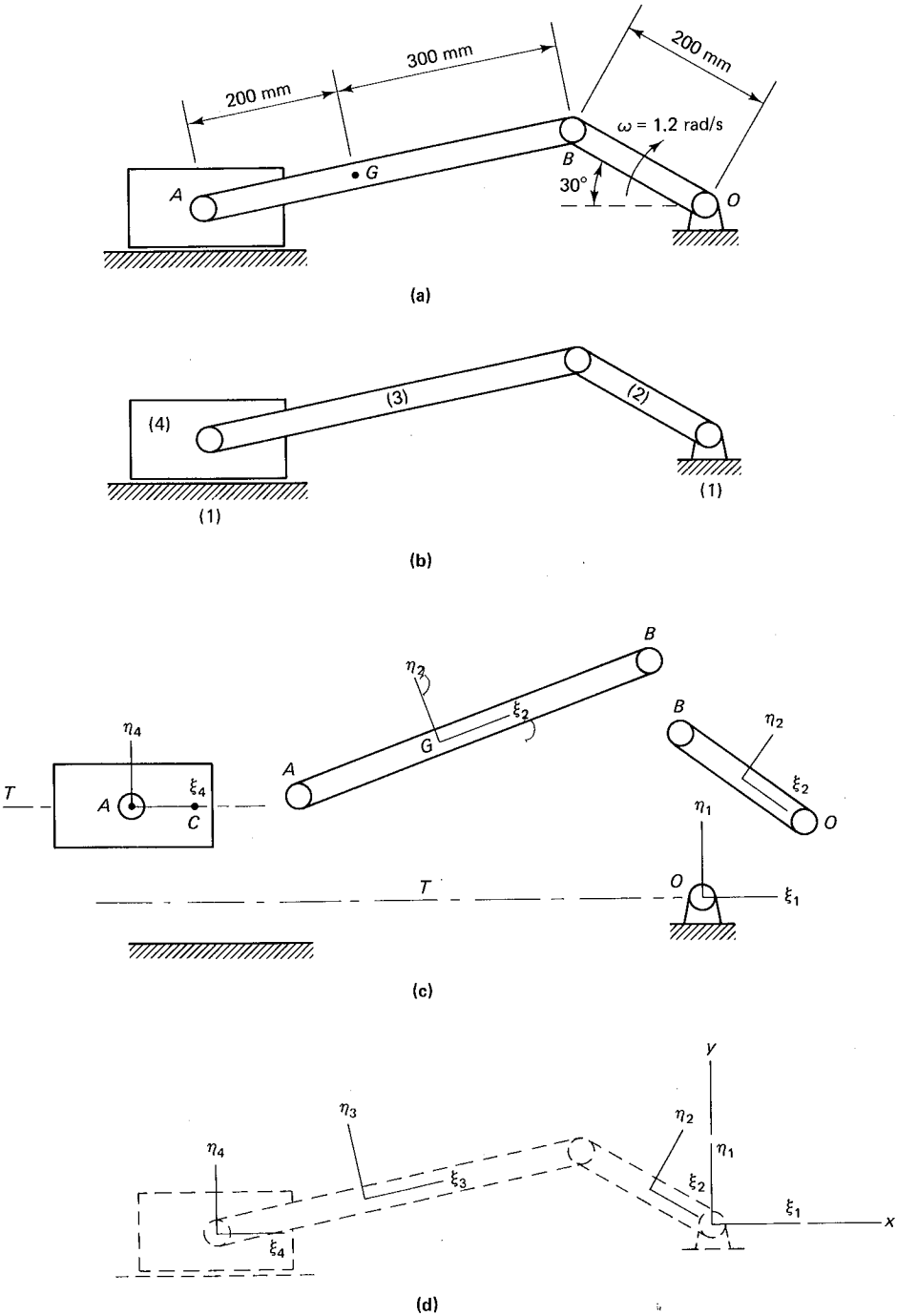

Figure 4.30 Kinematic modeling of a slider-crank mechanism.

tion. These points are A, C, and O. The distance AC is taken here as 100 mm. The data that define the translational joint constraints are as follows:

$$\begin{aligned} &\xi_4^A = 0.0, \qquad \eta_4^A = 0.0, \qquad \xi_4^C = 100.0, \qquad \eta_4^C = 0.0, \\ &\xi_1^0 = 0.0, \qquad \eta_1^0 = 0.0 \end{aligned} \tag{b}$$

Additional constraints are needed to ensure that body 1 is the nonmoving body. A global xy coordinate system is added to the configuration, as shown in Fig. 4.30(d). For convenience, the xy coordinate system is positioned to coincide with the $\xi_1\eta_1$ coordinates. Therefore, the conditions

$$x_1 = 0.0, \qquad y_1 = 0.0, \qquad \phi_1 = 0.0 \tag{c}$$

must be satisfied.

The driving constraint on ϕ_2 is written, using Eq. 4.36, as

$$\phi_2 - 5.76 + 1.2t = 0 \tag{d}$$

where 5.76 rad is equal to 360° − 30°. Since the crank rotates clockwise, a negative sign is selected for ω.

The data defined by Eqs. a through c are sufficient to describe the connectivity between different bodies in the system. If a computer program is available to generate all of the kinematic constraint equations, such as the program of Chap. 5, then the constraint equations are set up and analyzed automatically. Such a program requires an initial estimate of the coordinates of the system, which is used to start the Newton-Raphson iteration for position analysis. These estimates are found from Fig. 4.30(d) to be,

$$\begin{aligned} x_1 &= 0.0, & y_1 &= 0.0, & \phi_1 &= 0.0 \\ x_2 &= -86.6, & y_2 &= 50.0, & \phi_2 &= 5.76 \\ x_3 &= -380.5, & y_3 &= 40.0, & \phi_3 &= 0.2 \\ x_4 &= -663.1, & y_4 &= 0.0, & \phi_4 &= 0.0 \end{aligned} \tag{e}$$

These estimates need not be accurate. The Newton-Raphson algorithm starts the iterations using the estimated values and finds the exact values for the coordinates at $t = 0$. The estimates can be made by rough measurements from the actual system, or from an illustration by means of a ruler and protractor.

Since there are 12 coordinates in this problem, the computer program must generate 12 kinematic constraint equations. These equations can be obtained by substituting the data of Eqs. a to d in the constraint equations derived in the previous sections. Equation c yields three constraints:

$$\begin{aligned} \Phi_1 &\equiv x_1 = 0.0 \\ \Phi_2 &\equiv y_1 = 0.0 \\ \Phi_3 &\equiv \Phi_1 = 0.0 \end{aligned} \tag{f}$$

Substitution of Eq. a into the revolute-joint constraints of Eq. 4.9 yields six constraint equations for the three revolute joints:

$$\begin{aligned} \Phi_4 &\equiv x_4 - x_3 + 200 \cos \phi_3 = 0 \\ \Phi_5 &\equiv y_4 - y_3 + 200 \sin \phi_3 = 0 \\ \Phi_6 &\equiv x_3 + 300 \cos \phi_3 - x_2 + 100 \cos \phi_2 = 0 \\ \Phi_7 &\equiv y_3 + 300 \sin \phi_3 - y_2 + 100 \sin \phi_2 = 0 \end{aligned}$$

$$\Phi_8 \equiv x_2 + 100 \cos \phi_2 - x_1 = 0$$
$$\Phi_9 \equiv y_2 + 100 \sin \phi_2 - y_1 = 0$$

Two constraint equations for the translational joint are obtained by substituting the data of Eq. *b* into Eq. 4.12 and using Eq. 4.3:

$$\Phi_{10} \equiv (-100 \cos \phi_4)(y_1 - 100 \sin \phi_1 - y_4) - (x_1 - 100 \cos \phi_1 - x_4)(-100 \sin \phi_4) = 0$$

$$\Phi_{11} \equiv \phi_4 - \phi_1 = 0$$

Equation *d* is the driving constraint:

$$\Phi_{12} \equiv \phi_2 - 5.76 + 1.2t = 0$$

The nonzero entries of the Jacobian matrix for these 12 constraints are found from Table 4.2. The positions of these entries are shown in Fig. 4.31. There are 36 nonzero entries in the 12 × 12 matrix. The nonzero entries are:

$$1, 2, 3, 6, 10, 14, 18, 22, 26, 34, 36 = 1$$
$$4, 8, 12, 16, 20, 24, 35 = -1$$
$$5 = -200 \sin \phi_3$$
$$9 = 200 \cos \phi_3$$
$$13, 23 = -100 \sin \phi_2$$
$$15 = -300 \sin \phi_3$$
$$17, 27 = 100 \cos \phi_2$$
$$19 = 300 \cos \phi_3$$
$$28 = 100 \sin \phi_4$$
$$29 = -100 \cos \phi_4$$
$$30 = 10{,}000(\cos \phi_1 \cos \phi_4 + \sin \phi_1 \sin \phi_4)$$
$$31 = -28$$
$$32 = -29$$
$$33 = 100[\sin \phi_4 (y_1 - 100 \sin \phi_1 - y_4) + \cos \phi_4 (x_1 - 100 \cos \phi_1 - x_4)]$$

Note that some of the entries at any given instant of time, depending on the value of the coordinates, may become zero. This example illustrates that about 83 percent of the entries of this Jacobian matrix are exactly zero. Therefore, the matrix is said to be *sparse*.

4.4.2 Quick-Return Mechanism

Figure 4.32(a) shows a commonly used quick-return mechanism that produces a slow cutting stroke of a tool (attached to slider *D*) and a rapid return stroke. The driving crank *OA* turns at the constant rate of 3 rad/s. Several ways to model this mechanism are pre-

$$
\begin{array}{c}
 \\ \partial\Phi_1/\partial\ldots \\ \partial\Phi_2/\partial\ldots \\ \partial\Phi_3/\partial\ldots \\ \partial\Phi_4/\partial\ldots \\ \partial\Phi_5/\partial\ldots \\ \partial\Phi_6/\partial\ldots \\ \partial\Phi_7/\partial\ldots \\ \partial\Phi_8/\partial\ldots \\ \partial\Phi_9/\partial\ldots \\ \partial\Phi_{10}/\partial\ldots \\ \partial\Phi_{11}/\partial\ldots \\ \partial\Phi_{12}/\partial\ldots
\end{array}
\begin{array}{c}
\begin{array}{cccccccccccc}
x_1 & y_1 & \phi_1 & x_2 & y_2 & \phi_2 & x_3 & y_3 & \phi_3 & x_4 & y_4 & \phi_4
\end{array} \\
\begin{bmatrix}
1 & 0 & 0 & 0 & 0 & 0 & 0 & 0 & 0 & 0 & 0 & 0 \\
0 & 2 & 0 & 0 & 0 & 0 & 0 & 0 & 0 & 0 & 0 & 0 \\
0 & 0 & 3 & 0 & 0 & 0 & 0 & 0 & 0 & 0 & 0 & 0 \\
0 & 0 & 0 & 0 & 0 & 0 & 4 & 0 & 5 & 6 & 0 & 7 \\
0 & 0 & 0 & 0 & 0 & 0 & 0 & 8 & 9 & 0 & 10 & 11 \\
0 & 0 & 0 & 12 & 0 & 13 & 14 & 0 & 15 & 0 & 0 & 0 \\
0 & 0 & 0 & 0 & 16 & 17 & 0 & 18 & 19 & 0 & 0 & 0 \\
20 & 0 & 21 & 22 & 0 & 23 & 0 & 0 & 0 & 0 & 0 & 0 \\
0 & 24 & 25 & 0 & 26 & 27 & 0 & 0 & 0 & 0 & 0 & 0 \\
28 & 29 & 30 & 0 & 0 & 0 & 0 & 0 & 0 & 31 & 32 & 33 \\
0 & 0 & 34 & 0 & 0 & 0 & 0 & 0 & 0 & 0 & 0 & 35 \\
0 & 0 & 0 & 0 & 0 & 36 & 0 & 0 & 0 & 0 & 0 & 0
\end{bmatrix}
\end{array}
$$

Figure 4.31 Position of nonzero entries of the Jacobian matrix for the slider-crank mechanism.

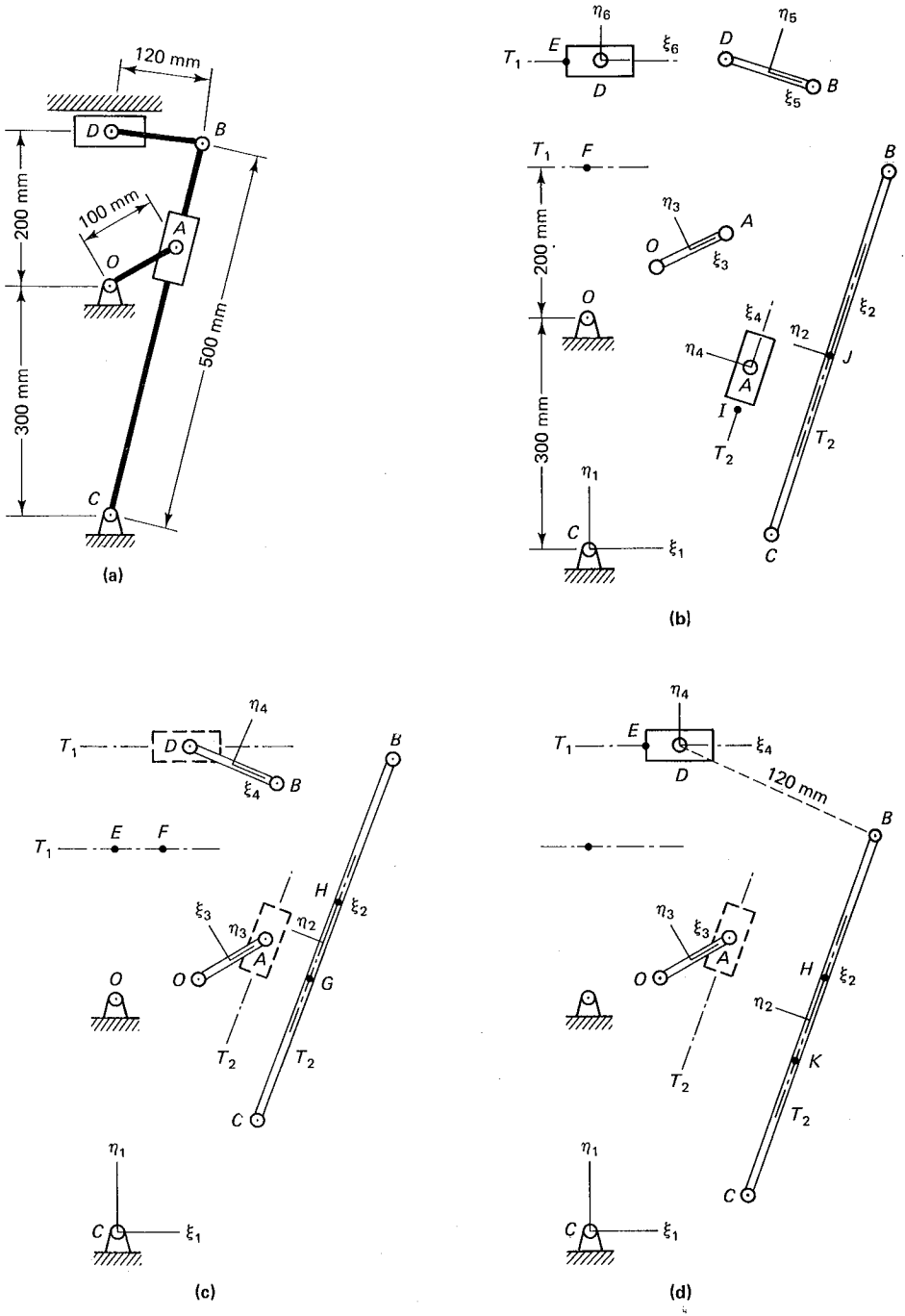

Figure 4.32 Kinematic modeling of a quick-return mechanism.

sented in this section. Each model has some advantage and some disadvantage in relation to the others.

Model 1. A maximum number of six bodies is used in the first model, as shown in Fig. 4.32(b). This model requires five revolute joints and two translational joints. There are 18 coordinates, 10 revolute-joint constraint equations, 4 translational-joint constraint equations, 3 ground constraints, and 1 driving constraint. Bodies are numbered as shown in Fig. 4.32(b), and the following data are deduced from this figure for the revolute and translational joints:

$$\left.\begin{array}{llll} \xi_3^A = 50, & \eta_3^A = 0, & \xi_4^A = 0, & \eta_4^A = 0 \\ \xi_2^B = 250, & \eta_2^B = 0, & \xi_5^B = 60, & \eta_5^B = 0 \\ \xi_1^C = 0, & \eta_1^C = 0, & \xi_2^C = -250, & \eta_2^C = 0 \\ \xi_5^D = -60, & \eta_5^D = 0, & \xi_6^D = 0, & \eta_6^D = 0 \\ \xi_1^0 = 0, & \eta_1^0 = 300, & \xi_3^0 = -50, & \eta_3^0 = 0 \end{array}\right\} \text{revolute joints}$$

$$\left.\begin{array}{llll} \xi_4^A = 0, & \eta_4^A = 0, & \xi_4^I = -10, & \eta_4^I = 0 \\ \xi_2^J = 0, & \eta_2^J = 0 & & \\ \xi_6^D = 0, & \eta_6^D = 0, & \xi_6^E = -10, & \eta_6^E = 0 \\ \xi_1^F = 0, & \eta_1^F = 500 & & \end{array}\right\} \text{translational joints}$$

To constrain body 1 to the ground, three conditions must be satisfied:

$$x_1 = 0, \qquad y_1 = -300, \qquad \phi_1 = 0$$

and the driving constraint may be written as

$$\phi_3 - 0.52 - 3t = 0$$

where it is assumed that the initial angle $\phi_3^0 = 30°$.

Model 2. In the second model, the two sliders, which were modeled as bodies 4 and 6 in model 1, are combined with the revolute joints at A and D. A total of four bodies, three revolute joints, and two revolute-translational joints are used in this model. The system has 12 coordinates, 6 revolute-joint constraints, 2 revolute-translational joint constraints, 3 ground constraints, and 1 driving constraint. This model is shown in Fig. 4.32(c), for which the following data can be obtained:

$$\left.\begin{array}{llll} \xi_2^B = 250, & \eta_2^B = 0, & \xi_4^B = 60, & \eta_4^B = 0 \\ \xi_1^C = 0, & \eta_1^C = 0, & \xi_2^C = -250, & \eta_2^C = 0 \\ \xi_1^0 = 0, & \eta_1^0 = 300, & \xi_3^0 = -50, & \eta_3^0 = 0 \end{array}\right\} \text{revolute joints}$$

$$\left.\begin{array}{llll} \xi_3^A = 50, & \eta_3^A = 0 & & \\ \xi_2^G = -10, & \eta_2^G = 0, & \xi_2^H = 15, & \eta_2^H = 0 \\ \xi_4^D = -60, & \eta_4^D = 0 & & \\ \xi_1^E = 0, & \eta_1^E = 500, & \xi_1^F = 10, & \eta_1^F = 500 \end{array}\right\} \text{revolute-translational joints}$$

Note that points E, F, G, and H are chosen on their corresponding lines of translation. The ground and driving constraints are modeled as in model 1.

One advantage of this model is that it has fewer coordinates than the first model. However, a disadvantage arises if an additional body is to be attached to the slider D. Since in this model the slider D is not modeled as a body, no other bodies may be attached to it.

Model 3. In model 3 the slider D is chosen as a body that slides relative to the frame with a translational joint. The link BD is modeled as a massless revolute-revolute joint. This model has a total of four bodies, two revolute joints, one translational joint, one revolute-revolute joint, and one revolute-translational joint. The data for this model can be derived from Fig. 4.32(d), as follows:

$$\left.\begin{array}{llll} \xi_1^C = 0, & \eta_1^C = 0, & \xi_2^C = -250, & \eta_2^C = 0 \\ \xi_1^O = 0, & \eta_1^O = 300, & \xi_3^O = -50, & \eta_3^O = 0 \end{array}\right\} \text{revolute joints}$$

$$\left.\begin{array}{llll} \xi_4^D = 0, & \eta_4^D = 0, & \xi_4^E = -10, & \eta_4^E = 0 \\ \xi_1^F = 0, & \eta_1^F = 500 & & \end{array}\right\} \text{translational joint}$$

$$\left.\begin{array}{llll} \xi_2^B = 250, & \eta_2^B = 0, & \xi_4^D = 0, & \eta_4^D = 0 \\ d = 120 & & & \end{array}\right\} \text{revolute-revolute joint}$$

$$\left.\begin{array}{llll} \xi_3^A = 50, & \eta_3^A = 0 & & \\ \xi_2^K = -10, & \eta_2^K = 0, & \xi_2^H = 15, & \eta_2^H = 0 \end{array}\right\} \text{revolute-translational joint}$$

The ground and driving constraints are modeled as in model 1.

$$\left.\begin{array}{llll} \xi_3^A = 50, & \eta_3^A = 0 & & \\ \xi_2^G = -10, & \eta_2^G = 0, & \xi_2^H = 15, & \eta_2^H = 0 \\ \xi_4^D = -60, & \eta_4^D = 0 & & \\ \xi_1^E = 0, & \eta_1^E = 500, & \xi_1^F = 10, & \eta_1^F = 500 \end{array}\right\} \text{revolute-translational joints}$$

$$\left.\begin{array}{llll} \xi_3^A = 50, & \eta_3^A = 0 & & \\ \xi_2^G = -10, & \eta_2^G = 0, & \xi_2^H = 15, & \eta_2^H = 0 \\ \xi_4^D = -60, & \eta_4^D = 0 & & \\ \xi_1^E = 0, & \eta_1^E = 500, & \xi_1^F = 10, & \eta_1^F = 500 \end{array}\right\} \text{revolute-translational joints}$$

This model has the advantage of a smaller number of coordinates than model 1, and since the slider at D is modeled as a body, it does not have the disadvantage of model 2. In none of these three models is the crank OA modeled by a massless revolute-revolute joint between points O and A. Since OA is the driving link, it must have its own coordinates for implementing the driving constraint.

PROBLEMS

4.1 Point C on body i has global coordinates $\mathbf{r}_i^C = [3.3, 2.3]^T$. (See Fig. P.4.1.) Attach a coordinate system to this body with its origin at C. Determine the vector of coordinates if $\alpha = 50°$. Also determine $\mathbf{s}'^P_i$ and $\mathbf{r}_i^P$ if $d = 1.2$.

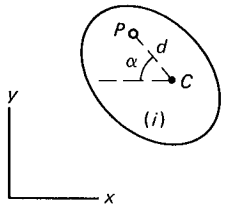

Figure P.4.1

4.2 If $\mathbf{r}_2 = [5, 2]^T$, $\phi_2 = 30°$, and $\mathbf{r}_2^Q = [6, 1.5]^T$, find the local coordinates of Q. (See Fig. P.4.2)

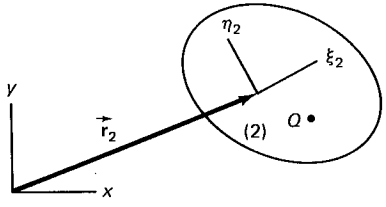

Figure P.4.2

4.3 Point P_i has local and global coordinates

$$\mathbf{s}'^P_i = \begin{bmatrix} 1.3 \\ -2.2 \end{bmatrix} \qquad \mathbf{r}_i^P = \begin{bmatrix} -1.7 \\ 0.5 \end{bmatrix}$$

Find the translational coordinates of body i if $\phi_i = 32°$. On graph paper, show the orientation of the local coordinate system with respect to the global coordinate system and locate point P.

4.4 The coordinates of body i are $\mathbf{r}_i = [3.2, 2.8]^T$ and $\phi_i = 80°$. Points A and B have local coordinates $\mathbf{s}'^A_i = [-1.1, -0.4]^T$ and $\mathbf{s}'^B_i = [1.9, 2.3]^T$. Point C has global coordinates $\mathbf{r}_i^C = [5.3, 4.0]^T$. Find the following:

(a) The global coordinates of A

(b) The global components $\mathbf{s}_i^B$

(c) The local coordinates of C

4.5 If Cartesian coordinates are used in constraint formulation, determine the following for each of the mechanisms shown in Fig. P.4.5:

(a) Number of bodies and coordinates

(b) Number of constraint equations

(c) Number of degrees of freedom

(d) Number of dependent and independent coordinates

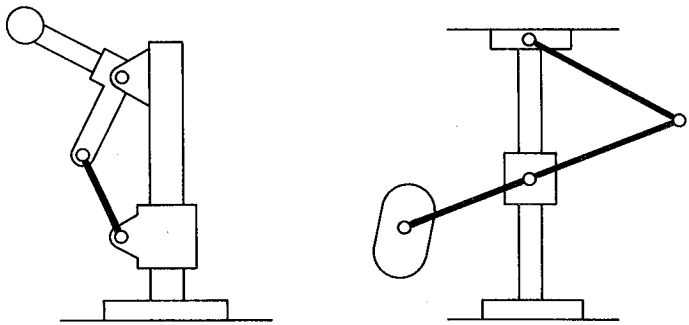

(a) (b)

Figure P.4.5

4.6 Determine the Jacobian matrix and write the velocity and acceleration equations for the constraint equations

$$\Phi_1 \equiv x_4 + 1.6 \cos \phi_4 - 0.3 \sin \phi_4 - x_1 + 0.75 \sin \phi_1 = 0$$
$$\Phi_2 \equiv y_4 + 1.6 \sin \phi_4 + 0.3 \cos \phi_4 - y_1 - 0.75 \cos \phi_1 = 0$$

4.7 Determine the minimum number of bodies and the types of joints required to model the mechanism shown in Fig. P.4.7. How many coordinates are involved?

4.8 Attach body-fixed coordinate systems to bodies 2 and 3 in Fig. P.4.8 with their origins at C_2 and C_3. Write constraint equations for this system in their simplest form.

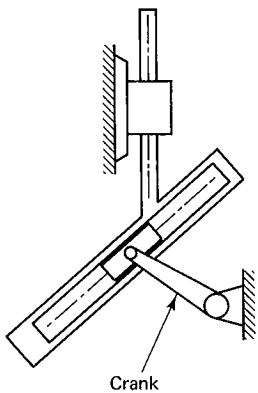

Figure P.4.7

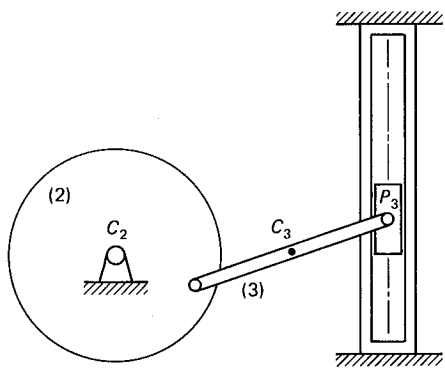

Figure P.4.8

4.9 Two vectors $\vec{s}_1$ and $\vec{s}_2$, attached to bodies 1 and 2, respectively, have local components $\mathbf{s}_1' = [1.2, -0.5]^T$ and $\mathbf{s}_2' = [-0.3, 0.8]^T$. Vector $\mathbf{q}$ is defined as $\mathbf{q} = [x_1, y_1, \phi_1, x_2, y_2, \phi_2]^T$.

(a) If $\phi_1 = 30°$ and $\phi_2 = 45°$, evaluate the entries of the Jacobian matrix $\Phi_{\mathbf{q}}$ for $\Phi \equiv \mathbf{s}_1^T\mathbf{s}_2$.

(b) If $x_1 = 6.2$, $y_1 = 1$, $\phi_1 = 30°$, $x_2 = -1.9$, $y_2 = 2.3$, and $\phi_2 = 45°$, evaluate the entries of the Jacobian matrix for $\mathbf{\Phi} \equiv \tilde{\mathbf{s}}_1\mathbf{d}$ where $\mathbf{d} = [x_2 - x_1, y_2 - y_1]^T$.

4.10 Revolute joints A and B have local coordinates $\mathbf{s}_1'^A = [0, 1.5]^T$, $\mathbf{s}_2'^A = [-2.2, 0]^T$, $\mathbf{s}_2'^B = [2.2, 0]^T$, and $\mathbf{s}_3'^B = [2, 0]^T$. (See Fig. P.4.10.) Coordinates of the moving bodies are estimated as $\mathbf{r}_1 = [-2, 2.5]^T$, $\phi_1 = -12°$, $\mathbf{r}_2 = [0.5, 3.6]^T$, $\phi_2 = -8°$, $\mathbf{r}_3 = [1.6, 1.7]^T$, and $\phi_3 = 56°$. Are the constraint equations for revolute joints A and B violated or not?

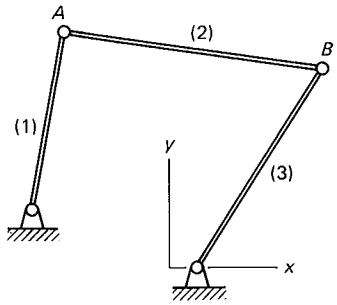

Figure P.4.10

4.11 For the translational joint shown in Fig. 4.5, use the vector product operation to derive the first constraint of Eq. 4.12.

4.12 For the revolute-translational joint shown in Fig. 4.9, use the vector product operation to derive the constraint of Eq. 4.16.

4.13 Since two bodies connected by a translational joint can translate relative to one another, it is possible for vector $\vec{d}$ to become a zero vector at some instant. Does this cause any numerical difficulty in kinematic analysis?

4.14 For the mechanism shown in Fig. P.4.14, link *ABE* is the crank. If only revolute- and translational-joint constraints are available, determine the number of bodies and the number of constraint equations needed to model this system. If, in addition, revolute-revolute and revolute-translational joint constraints are available, show different ways that the number of bodies and the number of constraints can be minimized.

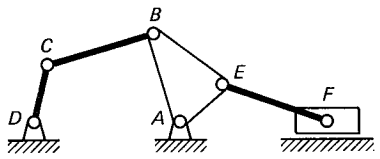

Figure P.4.14

4.15 Derive constraint equations for a rack and pinion where

(a) The rack moves on a translational joint with respect to the ground and the line of translation is not parallel to any of the coordinate axes.

(b) The rack and the pinion can translate and rotate with respect to the ground (general case).

4.16 If $\mathbf{g}_i' = [\mu, \nu]_i^T$ is tangent to a curve at a point P_i, show that $\mathbf{n}_i' = [-\nu, \mu]_i^T$ is normal to the curve at P_i. Then, modify the cam-follower constraints of Eq. 4.29 by using the normal vectors and vector product instead of the tangent vector and scalar product.

4.17 Most books on numerical methods provide algorithms and program listings for cubic spline functions. Experiment with one of these algorithms and try to determine values of a function and its first and second derivatives at randomly specified points. The program can later be used to expand the capabilities of the kinematic and dynamic analysis programs listed in Chaps. 5 and 10.

4.18 Derive constraint equations for each of the cam-follower pairs shown in Fig. P.4.18.

4.19 Simplify the general formulation of constraint equations for the cam-follower pairs shown in Fig. P.4.19. For (a) and (b) the contacting surface of the cam is a sine function, and for (c), (d), and (e) the cam has a circular outline.

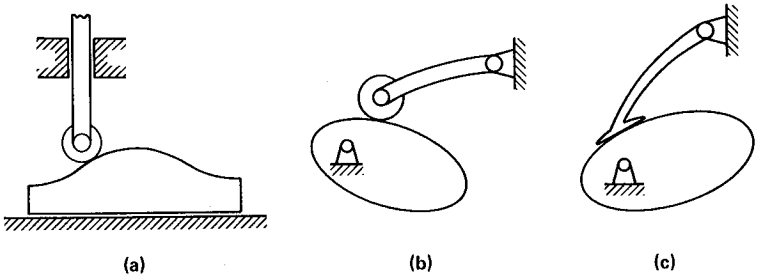

Figure P.4.18

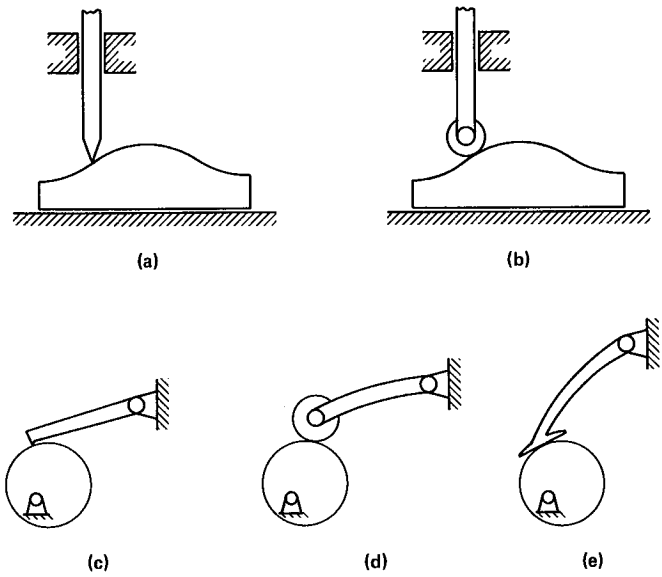

Figure P.4.19

4.20 Verify the entries of the Jacobian matrix and vector γ listed in Tables 4.2 and 4.3.

4.21 Derive expressions for the entries of the Jacobian matrix and vector γ for the spur gear constraint of Eq. 4.18.

4.22 Derive expressions for the entries of the Jacobian matrix and vector γ for the cam-follower constraints of Eq. 4.27. Note that the Jacobian matrix must contain an additional column associated with the artificial coordinate θ_i.

4.23 What is the size of the Jacobian matrix for a four-bar mechanism modeled by four bodies and four revolute joints? Show the location of the nonzero entries in this matrix. What percentage of the elements of the matrix are nonzero elements?

4.24 Derive constraint equations to keep the translational speed of a body constant along a known direction denoted by a unit vector $\vec{u}$. Consider two cases:

(a) Vector $\vec{u}$ is fixed to the global coordinate system.

(b) Vector $\vec{u}$ is fixed to the body coordinate system.